TRENDS IN SCIENCES 2025; 22(10): 10855
https://doi.org/10.48048/tis.2025.10855
REVIEW ARTICLE

Phenolic Derivatives from Meliaceae Family and Their Biological Activities

Hikma Ainazzahra[1], Citra Nisa Ul Inayah[1], Al Arofatus Naini[2], Kindi Farabi[1,3], Desi Harneti[1] and Unang Supratman[1,3,*]

[1]Department of Chemistry, Faculty of Mathematics and Natural Sciences, Universitas Padjadjaran, West Java 45363, Indonesia
[2]Research Center for Pharmaceutical Ingredients and Traditional Medicine, National Research and Innovation Agency (BRIN), Cibinong Science Center Complex - BRIN, West Java 16911, Indonesia
[3]Central Laboratory, Universitas Padjadjaran, West Java 45363, Indonesia

([*]Corresponding author's e-mail: unang.supratman@unpad.ac.id)

Received: 5 June 2025, Revised: 4 July 2025, Accepted: 11 July 2025, Published: 5 August 2025

Abstract

Phenolic compounds are an important class of secondary metabolites found in the Meliaceae family, which is widely distributed in tropical and subtropical regions. This study presents a comprehensive review of 73 scientific publications from 1985 to 2024, focusing on the occurrence, classification, and biological activities of phenolic compounds isolated from various plant parts such as leaves, barks, seeds, roots, fruits, and flowers. A total of 147 phenolic compounds were identified, categorized into major groups including simple phenolics, coumarins, stilbenes, flavonoids, and lignans. Lignans were the most abundant class, accounting for 45.6% of the total compounds reported. These phenolic constituents exhibit a wide range of biological activities, such as antioxidant, anti-inflammatory, antimicrobial, anticancer, and agonistic activity. Notably, several lignans, such as methyl rocaglate and its derivatives, displayed potent cytotoxicity in the nanomolar range (IC_{50} = 0.0023 - 0.068 µM), highlighting their potential as anticancer agents. Data were collected and analyzed using established scientific databases including PubMed, Scopus, Reaxys, and SciFinder. The findings underscore the rich chemical diversity and therapeutic potential of Meliaceae-derived phenolics, particularly lignans, as promising candidates for pharmaceutical development. Further pharmacological and clinical investigations are recommended to validate their efficacy and safety.

Keywords: Meliaceae, Phenolic, Secondary metabolites, Bioactive compounds

Introduction

Meliaceae, commonly known as the mahogany family, comprises flowering plants ranging from large trees to shrubs, classified under the order Sapindales. This family encompasses 740 species across 58 genera, distributed throughout the Malayan-Indo region, Africa-Madagascar, and Australia-Asia [1]. Phytochemical investigations of this family have revealed limonoids [2] and terpenoids [3,4] as the major chemical constituents, possessing broad and potent biological activities [5-7]. Additionally, naturally occurring phenolic derivatives from Meliaceae family were also fequently reported amounts of flavonoids and phenolic compounds are found in genus such as *Cedrela*, *Aglaia*, *Dysoxylum*, and *Melia* [8-11]. Reported to have potential biological activities, including antioxidant [12], cytotoxic [13], and antimicrobial [14], inflammatory [9], and serotonin receptor agonistic [11], making them valuable for various therapeutic applications.

Phenolic compounds constitute a major group of secondary metabolites in plants, characterized by structural diversity. Chemically, phenolics are defined by the presence of at least 1 aromatic ring bearing hydroxyl groups. The major classes of phenolic compounds include flavonoids (e.g., catechins, anthocyanins), phenolic acids (e.g., gallic acid, ellagic acid), stilbenes (e.g., resveratrol), lignans, and non-

flavonoid compounds such as curcumin [16]. The diverse substitution patterns on the phenol core structure result in a wide variety of phenolic structures. These phytochemicals are present in nutritional sources and herbal medicines, with flavonoids and numerous other phenolics reported to exhibit potent antioxidant, anticancer, antimicrobial, anti-inflammatory, and agonistic [17-19].

To date, no literature review has specifically focused on providing comprehensive information regarding the occurrence of phenolic derivatives within the Meliaceae family, including their distribution, structural diversity, and biological activities. Therefore, it is imperative to develop a thorough summary encompassing the chemical and biological aspects of these compounds. This study presents the 1st comprehensive review, covering a total of 147 phenolic compounds and their derivatives, categorized by their core structures, types, and biological activities. This review provides an overview of the possible biogenetic pathways for each phenolic type, highlights their structural differences, and discusses the potential of Meliaceae-derived phenolics as promising candidates for drug discovery. It is expected to serve as a preliminary foundation for future studies in the development of novel therapeutics.

Method and materials

The literature search in this review was conducted systematically using major scientific databases, including Scopus, ScienceDirect, PubMed, and Google Scholar. The search focused on studies published between 1985 and April 2024, using a combination of relevant keywords such as “Phenolic compounds from Meliaceae”, “Coumarins from Meliaceae”, “Stilbenes from Meliaceae”, “Flavonoids from Meliaceae”, and “Lignans from Meliaceae”, among others. Articles were manually screened through a comprehensive evaluation of titles, abstracts, and full texts to ensure relevance to the review topic.

Inclusion criteria were applied to select original research articles (excluding reviews) that reported the isolation of pure phenolic compounds from plants belonging to the Meliaceae family. Articles were included if they provided spectroscopic data (e.g., NMR, MS, UV, IR) supporting structural elucidation, along with information on biological activities (e.g., cytotoxic, antioxidant, or antibacterial activities). In contrast, articles classified as reviews, editorials, or letters to the editor; studies focusing solely on crude extract activity without isolation of pure compounds; and non-English publications were excluded.

From an initial pool of over 500 publications, a total of 74 articles were selected based on the predefined inclusion criteria. Data from each selected study were systematically extracted, including compound names, plant sources, types of phenolic compounds, and available bioactivity data. All information was recorded in a structured data extraction sheet to ensure consistency and accuracy. Each compound was cross-verified using Reaxys and SciFinder to confirm chemical identity and structure, and to eliminate redundancy. Data extraction and validation were conducted independently by 2 authors to minimize errors and enhance the reliability of the review.

Phytochemistry

The reviewed data covers a total of 17 genera within the Meliaceae family. The genus *Aglaia* was the most frequently reported, represented by multiple species including *A. andamanica*, *A. elaeagnoidea*, *A. elliptica*, *A. eximia*, *A. odorata*, and *A. testicularis*. The genus *Amoora* included 2 species: *A. cucullata* and *A. rohituka*, while *Aphanamixis* was represented solely by *A. polystachya*. The genus *Azadirachta* included *A. indica*, and *Cedrela* comprised *C. serrata* and *C. sinensis*. From *Chisocheton*, only *C. penduliflorus* was identified, and from *Dysoxylum*, the species *D. lenticellare* was recorded. Moreover, the genus *Ekebergia* included several species, namely *E. benguelensis*, *E. capensis*, and *E. senegalensis*. *Entandrophragma* was represented by a single species, *E. utile*, while *Guarea* included *G. macrophylla* and *G. rhophalocarpa*. The genus *Melia* consisted of 2 frequently cited species, *M. azedarach* and *M. toosendan*. The genus *Pseudo Cedrela* was represented by *P. kotschyi*, and *Swietenia* by *S. mahagoni*. From *Toona*, only *T. sinensis* was included. The genus *Trichilia* contributed 3 species: *T. catigua*, *T. estipulata*, and *T. heudelotti*. Lastly, *Walsura* (*W. robusta*), and *Xylocarpus* (*X. granatum*) were each represented by a single species. This wide taxonomic distribution highlights the chemical diversity within the Meliaceae family, particularly the presence of phenolic compounds

across various genera, which forms the basis of the present review.

"Phenolic compounds" is a generic term that refers to a large number of compounds (more than 8,000) widely dispersed throughout the plant kingdom and characterized by having at least 1 aromatic ring with one or more hydroxyl groups attached. Phenolics are produced in plants as secondary metabolites via the shikimic acid pathway, primarily involving the enzyme phenylalanine ammonia-lyase (PAL) [16].

Phenolic compounds are broadly categorized into 2 primary groups: Flavonoids and non-flavonoids. Flavonoids possess a characteristic structure composed of 2 phenyl rings linked by a central pyran ring, and they can occur either in a free state or bound to sugar units. When the attached sugar is glucose, the compound is known as a glucoside; if the sugar is other than glucose, it is referred to more generally as a glycoside. In contrast, aglycones are the non-sugar-bound forms. Aglycones possess a flavylium ion (2-phenylbenzopyrilium), featuring a positively charged structure comprising a benzopyrilium core and a phenolic ring [16]. As shown in **Figure 1**, flavonoids in Meliaceae are subdivided into 4 subclasses: Flavonols, flavanones, flavanols, and flavones. Non-flavonoids are subdivided in 4 subclasses: Simple phenolic (e.g., phenolic acids, gallotannins, phenylpropanoids), coumarins, stilbenes, and lignans.

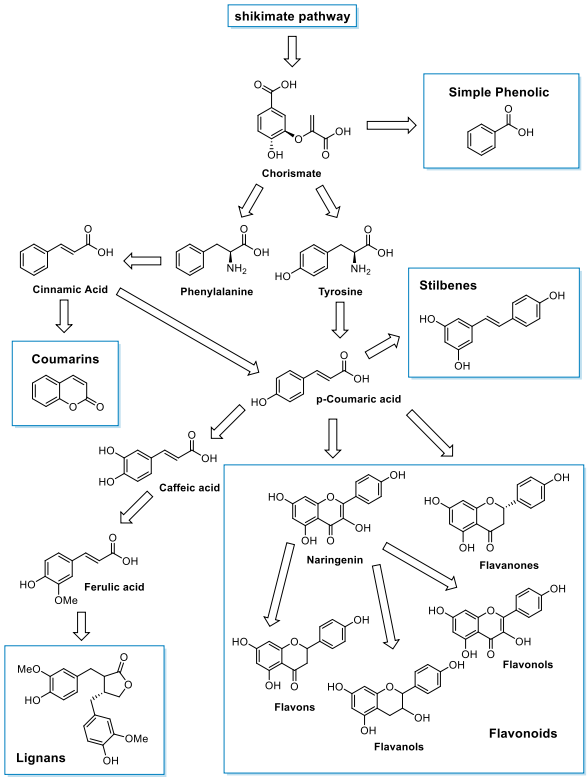

Figure 1 Biosynthesis of derivatives phenolic compound.

Literature collected from 1985 to 2024 revealed a total of 147 phenolic derivatives isolated from the leaves, fruits, stem bark, and twigs of the Meliaceae family. This review delineates the classification of phenolic derivatives in accordance with the sequential order of their biosynthetic pathways, including simple phenolics, coumarins, stilbenes, flavonoids, and lignans. Based on **Figure 2**, the lignans are the largest phenolic derivatives, with a total of 68 compounds (46.3%), followed by the flavonoid (32%), simple phenolic (12.2%), coumarin (6.8%), and stilbenes (2.7%). Meanwhile, **Figure 1** illustrates the relationship between biosynthetic pathways and the structural differences among phenolic compound classes within the Meliaceae family.

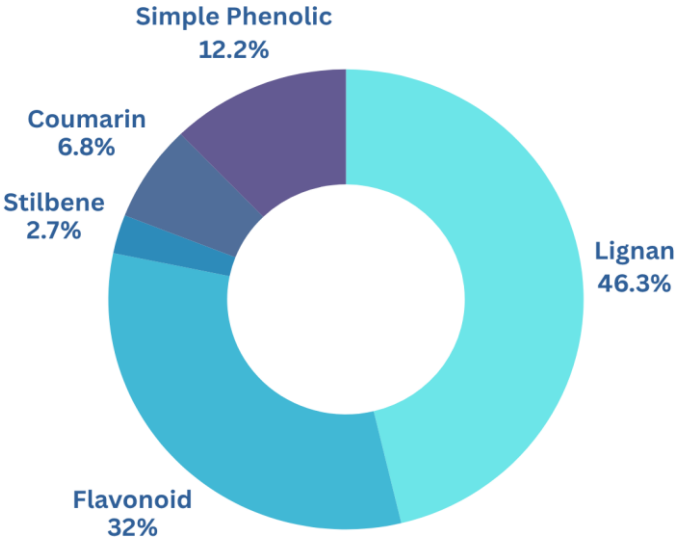

Figure 2 The distribution of phenolic derivatives isolated from the Meliaceae family.

Simple phenolic

The simple phenolic group comprises compounds characterized by a basic aromatic scaffold substituted with hydroxyl, methoxyl, or carboxyl-derived functional groups, and frequently conjugated with sugars, particularly glucose. This group is associated with non-cyclized C6-C1 compounds, in contrast to coumarins. This group consists phenolic acid, gallotannins, and phenylpropanoid derivatives. Phenolic acids derivatives comprise 4-hydroxybenzoic acid (1), vanillic acid (2), 4-hydroxy-3,5-dimethylbenzoic acid (3), gallic acid (4), protocatechuic acid (5), 2-methylprotocatechuic acid (6), atraric acid (7), (*E*)-4-hydroxycinnamic acid (8), 2-propionoxy-β-resorcylic acid (9), and trigallic acid (10). These compounds have been reported from various plant parts of Meliaceae family members, including the leaves of *Trichilia heudelotti*, *Toona sinensis*, and *Chisocheton penduliflorus*, the stem bark of *Ekebergia senegalensis* and *E. capensis*, and the seeds of *Xylocarpus granatum* [17,21-24]. These phenolic acid derivatives feature a phenolic core bearing hydroxyl and carboxyl groups, and their biosynthesis proceeds via the shikimate and phenylpropanoid pathways, involving oxidation, hydroxylation, methylation, and esterification reactions. Methyl gallate (14), a methylated derivative of gallic acid formed via carboxyl group methylation, is also found in *T. sinensis* [25]. In contrast, 3,4,5-trimethoxyphenyl β-D-glucopyranoside (12), obtained from the leaves and twigs of *Walsura robusta Roxb.*, is a glycosylated trimethoxybenzene derivative. This compound arises from stepwise methylation of gallic acid via *O*-methyltransferase, followed by glycosylation of the aromatic ring [26].

Furthermore, galloylglucose derivatives demonstrate increasing complexity in galloylation patterns on the glucose hydroxyl groups, including 6-*O*-galloyl-D-glucose (13), 1,2,3,6-tetra-*O*-galloyl-β-D-glucopyranose (15), 1,2,3,4,6-penta-*O*-galloyl-β-D-glucopyranose (16), and 1,2,3-tri-*O*-galloyl-β-D-glucopyranose (18), all of which were isolated from the leaves and shoots of *T. sinensis* [25]. These compounds are biosynthesized stepwise through the action of galloyltransferase enzymes on glucose substrates bearing free hydroxyl groups.

Subsequently, there are phenylpropanoid derivatives, senegalin (11), isolated from the stem bark of *Ekebergia senegalensis* [21], is a phenolic compound containing hydroxyl and possibly alkyl substituents on its aromatic ring. It is presumably biosynthesized via the phenylpropanoid pathway, involving phenylalanine deamination followed by oxidative transformation. In contrast, compound 17, (+)-ent-ficusol, isolated from the leaves of *Aglaia odorata Lour.* [29], is a phenylpropanoid derivative featuring hydroxyl, methoxy, and additional functional moieties, indicating the involvement of methyltransferases and oxidases in its biosynthetic route. Compound 17 represents a phenylpropanoate derivative identified as a methyl ester of hydroxyferulic acid, bearing a secondary hydroxyl group on the side chain and *ortho*-positioned hydroxyl and methoxy substituents on the aromatic ring.

Coumarin

The coumarins and hydroxycoumarins are synthesized from *trans*-p-coumaric acid and *trans*-cinnamic acid in plants. Coumarin represents an important class of oxygenated heterocyclic compounds biosynthetically derived from the phenylpropanoid pathway. Within this group, various structural modifications such as hydroxylation, methylation, and aromatic side-chain extension contribute to the chemical diversity and biological functionality of these compounds. One of the most well-known coumarins, scopoletin (19), a 6-methoxy-7-hydroxy derivative, was isolated from the leaves of *Guarea rhophalocarp*, the twigs of *Amoora dasyclada*, and the woods of *Trichilia Lepidota* [21,69,70]. This compound is biosynthesized from ferulic acid via ortho-hydroxylation and lactonization, followed by methylation at the C-6 position catalyzed by *O*-methyltransferase. Scoparone (23), a dimethylated derivative of scopoletin, was found in the wood and leaves of *Chisocheton penduliflorus* [22] and arises from further methylation of the hydroxyl group using S-adenosylmethionine (SAM) as the methyl donor.

Several other compounds exhibit more complex substitution patterns. For example, 4,6-dimethoxy-5-methylcoumarin (20), 6-hydroxy-4-methoxy-5-methylcoumarin (21), and 5-(hydroxymethyl)-4-methoxycoumarin (22) were isolated from the stem bark of *Ekebergia senegalensis*, *E. capensis* and the root bark of *E. benguelensis* [21,71,73] and exhibit variations in methyl, methoxy, and hydroxyl groups at positions 4 - 6 of the coumarin core. A simpler structure, 4-methoxy-5-methylcoumarin (24), found in the bark of *Ekebergia capensis* and *E. senegalensis* [23], may serve as a biosynthetic intermediate. In contrast, ekersenin (pereflorin) (25), isolated from the stem bark of *Ekebergia capensis* [73], displays a more lipophilic substitution pattern with methyl and methoxy groups at positions 4, 6, and 7.

A structurally distinct coumarin, 5-(4-hydroxyphenethenyl)-4,7-dimethoxycoumarin (26), isolated from the root bark of *Ekebergia benguelensis* [30], features an aromatic moiety with an ethylene linkage at C-5. Such structures are likely formed via condensation between a coumarin nucleus and phenylpropanoid precursors such as tyrosol or cinnamic acid derivatives, catalyzed by enzymes like prenyltransferases. Finally, 3,4-dihydro-4,4,5,8-tetramethylcoumarin (27) and 3,4-dihydro-4,4,7,8-tetramethylcoumarin-6-ol (28), both isolated from the fruits of *Azadirachta indica* [29], represent dihydrocoumarin derivatives characterized by reduction of the α,β-double bond at C-3 and C-4.

Stilbene

The stilbene group comprises phenolic compounds characterized by the presence of an ethenyl (-CH=CH-) bridge linking 2 aromatic rings. Within the Meliaceae family, stilbene derivatives have been specifically reported from *Ekebergia benguelensis*, all of which were isolated from the root bark of the plant. A total of 4 compounds (29 - 32) have been identified, namely (5-[(1*E*)-2-(4-hydroxyphenyl)ethenyl]-4,7-dimethoxy-3-methyl-2H-1-benzopyran-2-one), (5-[(1*E*)-2-(4-D-glucopyranosyloxyphenyl)ethenyl]-4,7-dimethoxy-3-methyl-2H-1-benzopyran-2-one), (1-{2-hydroxy-6-[(1*E*)-2-(4-hydroxyphenyl)ethenyl]-4-methoxyphenyl}-2-methyl-1-propanone), and (1-{2,4-dihydroxy-6-[(1*E*)-2-(4-hydroxyphenyl)ethenyl]-phenyl}-2-methyl-1-propanone). These compounds share a stilbene backbone that is structurally modified by methoxy and hydroxy substituents, notably, compound 30 also features glycosylation on the aromatic ring [30].

Flavonoid

Flavonoids are typically stored in the vacuoles of plant cells as glycosides. Structurally, they possess a basic skeleton consisting of 3 rings (C6-C3-C6), commonly labeled as rings A - C (**Figure 3**) [16]. Based on structural differences, flavonoids are generally classified into 7 subclasses, flavonols, flavones, isoflavones, anthocyanidins, flavanones, flavanols, and chalcones. This classification method is based on the oxidation degree of the central heterocycle. The sites of methyl and hydroxyl groups on the other 2 rings lead to various flavonoid glycoside modifications such as glycosylation and acylation.

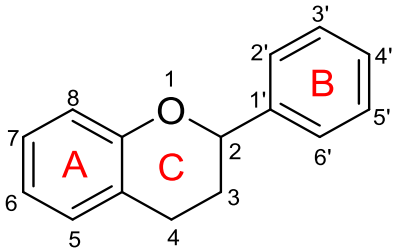

Figure 3 Basic skeleton of flavonoid.

The 1st subclass of flavonoids identified in the Meliaceae family is flavanones. Flavanones, also referred to as dihydroflavones, are characterized by a saturated C-ring, specifically lacking the double bond between the C2 and C3 positions. Basic flavanone structures such as catechin (33) from the leaves of *Swietenia mahagoni* [31] and 3,4′,5,7-tetrahydroxyflavanone (34) from the seeds of *Xylocarpus granatum* [24] represent simple flavonoids that can undergo various structural modifications. A diverse series of prenylated and methylated flavanones has been isolated from the flowers of *Azadirachta indica var. siamensis*, including euchrestaflavanone A (35), 4′-*O*-methylespedezaflavanone C (36), 3′-(3-hydroxy-3-methylbutyl)naringenin (37), 8-prenylnaringenin (38), 4′-*O*-methyl-8-prenylnaringenin (39), and 3′-prenyl naringenin (40) [32], reflecting the strong prenyltransferase activity exhibited by this species.

In the Meliaceae family, the most frequently encountered flavonoid subclass is flavonols. Flavonols, also known as 3-hydroxyflavones, are distinguished by specific substitution patterns on the A and B rings, which are connected through a 3-carbon bridge. These compounds are typically biosynthesized through the phenylpropanoid and acetate-malonate pathways, involving key enzymes such as chalcone synthase, flavonol synthase, and various transferases. Typically, the hydroxylation occurs at the 5 and 7 positions of the A ring, while the 3-position on the central C-ring is also hydroxylated, a feature that differentiates flavonols from other flavonoid subclasses. Based on their structural backbone, flavonols in Meliaceae can be broadly categorized into several groups, including kaempferol, quercetin, myricetin, and galangin derivatives.

Kaempferol (41) and quercetin (42) are fundamental flavonols widely distributed across the plant kingdom. In the Meliaceae family, kaempferol has been isolated from the stem bark of *Aglaia eximia* [33], while quercetin was identified in the roots of *Pseudocedrela kotschyi* [34]. Both compounds possess a hydroxyl group at the C-3 position and display characteristic B-ring substitution patterns—kaempferol with a hydroxyl at C-4′, and quercetin with hydroxyls at C-3′ and C-4′.

Several methylated derivatives of quercetin exhibit further structural diversification. Compounds such as 8-C-methyl quercetin (43) and 8-C-methyl-quercetin-5,7,3′,4′-tetramethyl ether (44), isolated from the roots of *Amoora rohituka* [35], feature uncommon C-methylation at the C-8 position, suggesting the action of specific prenyl/methyltransferases. In addition, *O*-methylation of hydroxyl groups yields ether derivatives, which can significantly affect solubility and metabolic stability. The compound 3,4′,7-trimethyl ester (45), also obtained from *Pseudocedrela kotschyi* [34], exhibits selective esterification at key hydroxyl positions. Kaempferide (46), a 4′-methoxy derivative of kaempferol, was identified in the flowers of *Azadirachta indica* var. *siamensis* [32]. Its selective methylation at the 4′ position of the B ring indicates the involvement of *O*-methyltransferases with regioselectivity toward aromatic hydroxyl groups. Another flavonol, 3-*O*-methyl mearnsetin (47), from the same species, shows methoxylation at the C-3 position. Highly hydroxylated flavonols, such as 3,6,8-trihydroxy-2-(3,4-dihydroxyphenyl)-4H-chromen-4-one (48), isolated from *Pseudocedrela kotschyi* roots [34], exhibit multiple hydroxyl substitutions across both A and B rings. Furthermore, 3-methoxy-3′-prenylkaempferol (49), also isolated from the flowers of *Azadirachta indica* var. *siamensis* [32], represents a prenylated flavonol bearing a methoxy group at the C-3 position and a prenyl group at C-3′ of the B ring. This dual

modification is indicative of the coordinated activity of *O*-methyltransferases.

Glycosylated derivatives of kaempferol constitute a major group of flavonols widely distributed among various Meliaceae species, with sugar substitution patterns that significantly influence their chemical properties and biological activities. Kaempferol-3-*O*-β-D-glucopyranoside (50), isolated from the leaves of *Aglaia andamanica* and *Ekebergia capensis* [36,72], and kaempferol-7-*O*-β-D-glucopyranoside (51) from *Guarea macrophylla* [37] demonstrate variation in glycosylation sites at the C-3 and C-7 positions, respectively. Additional glycosylated derivatives have been reported in the leaves of *Cedrela serrata*, including kaempferol-3-*O*-β-galactoside (trifolin, 54), kaempferol-3-*O*-β-glucoside (astragalin, 55), and the disaccharide-linked kaempferol-3-*O*-glucosyl-(1→2)-rutinoside (57) [8], highlighting the structural complexity introduced by extended sugar chains.

Among compounds isolated from *Toona sinensis*, kaempferol-3-*O*-L-arabinopyranoside (juglalin, 61) was identified [25], indicating glycosylation with arabinose. In *Melia azedarach*, kaempferol derivatives such as kaempferol-3-*O*-rhamnoside (63) and kaempferol-3-*O*-rutinoside (64) were reported [27]. The stem bark of *Aglaia eximia* yielded kaempferol-3-*O*-α-L-rhamnoside (66) and a diglycoside, kaempferol-3-*O*-β-D-glucosyl-α-L-rhamnoside (67) [33], suggesting the involvement of multiple glycosyltransferases in their biosynthesis. Furthermore, the compound kaempferol-3-*O*-rhamnosyl-(1→6)-(4″-trans-p-coumaroyl)-galactoside (69), isolated from *C. serrata* [8], incorporates a phenylpropanoid acyl moiety, further enhancing structural diversity and potential bioactivity.

Quercetin-based glycosylated flavonols are also widely represented, particularly in the leaves of *C. serrata* and *E. Capensis* with examples including quercetin-3-*O*-α-rhamnoside (52) and quercetin-3-*O*-β-D-glucopyranoside (isoquercitrin, 53) [8,72]. Additional derivatives such as quercetin-3-*O*-β-galactoside (hyperoside, 60) have also been identified in these species [8]. Quercetin-3-*O*-glucoside (56) has been reported in the leaves of *Swietenia mahagoni* [31], while *Toona sinensis* contains quercetin-3-*O*-α-L-rhamnopyranoside (58) and rutin (59), a disaccharide-linked derivative [25]. In *Melia azedarach*, quercetin-3-O-rutinoside (65) was identified along with a highly complex triglycoside, quercetin-3-O-[(rhamnosyl-1→6)-(4″-lactoyl-glucoside)]-4′-*O*-glucoside (68), which features both lactoyl acylation and multiple glycosylation events. In addition to quercetin derivatives, other glycosylated flavonols such as quercetin-3-*O*-β-D-galactopyranoside (62), identified in *Guarea macrophylla* [37], also contribute to the structural diversity of glycosylated flavonols, albeit still based on the quercetin backbone.

Flavones represent a subclass of flavonoids characterized by a 2-phenylchromen-4-one backbone lacking a hydroxyl group at the C-3 position. These compounds are biosynthesized via the phenylpropanoid-polyketide pathway and exhibit structural diversity through various modifications, including hydroxylation, methylation, glycosylation, and dimerization. Several *O*-methylated flavones have been isolated from the leaves of *Aglaia andamanica*, including 5-hydroxy-3,4′,7-trimethoxyflavone (70), retusin (71), and pachypodol (72) [36]. These compounds display methoxy group substitutions on both A and B rings, which enhance lipophilicity and improve metabolic stability by increasing resistance to enzymatic degradation. Such methylated derivatives are typically formed through the action of O-methyltransferases that transfer methyl groups from S-adenosylmethionine (SAM) to hydroxylated flavone precursors. Simple hydroxylated flavones such as chrysin (73) and apigenin (74) have been reported from the leaves of *Amoora cucullata* [20]. These compounds serve as biosynthetic precursors for a variety of other flavonoids and are recognized for their potent antioxidant and anti-inflammatory activities. The presence of a hydroxyl group at the C-4′ position in apigenin, absent in chrysin, significantly influences their polarity and biological activity profiles. A complex flavone glycoside, 8-C-methyl-5,7,3′,4′-tetrahydroxyflavone-3-*O*-β-D-xylopyranoside (75), was isolated from the roots of *Amoora rohituka* [35]. This compound combines hydroxylation, methylation, and glycosylation modifications, featuring a C-3 *O*-glycosidic linkage with a xylose moiety. Such structural complexity potentially enhances its pharmacological properties, particularly as a water-soluble antioxidant with improved stability in biological systems.

The biflavone class is represented by robustaflavone 4′,7″-dimethyl ether (76), identified in

the leaves of *Dysoxylum lenticellare* [39]. This compound results from the dimerization of 2 flavone units connected via a carbon-carbon (C–C) bridge, with methylation at positions 4′ and 7″ modulating its hydrophobic interactions and binding affinity toward protein targets. Additionally, the aglaodoratin series—aglaodoratin A (1), B (2), and C (3) (77-79)—isolated from the leaves of *Aglaia odorata Lour.* [9], exemplify the unique flavone structures characteristic of the *Aglaia* genus. These compounds have been closely associated with pronounced cytotoxic activity against cancer cell lines, highlighting their potential as anticancer agents.

Lignan

Lignans and neolignans constitute a major class of naturally occurring phenolic compounds widely distributed across the plant kingdom, including the Meliaceae family. Lignans are a class of natural phenolic compounds biosynthesized via the shikimic acid pathway and are formed through the oxidative dimerization of 2 phenylpropanoid (C6-C3) units. They are classified based on the mode of coupling: When the linkage is between positions C8 and C8′, the compounds are considered true lignans, whereas other coupling modes (e.g., C8-C3′, C3-O-C′) define neolignans [40]. Norlignans are a related group of natural products, commonly co-occurring with lignans or neolignans, and typically possess a C_{16} to C_{17} carbon skeleton. From a biosynthetic perspective, these compounds are likely derived from 2 arylpropanoid units with the loss of 1 or 2 carbon atoms, potentially via decarboxylation processes [40].

As illustrated in **Figure 4**, lignans are classified into 8 structural types based on their carbon skeletons, oxygen incorporation patterns, and cyclization modes. These categories include arylnaphthalene, aryltetralin, dibenzocyclooctadiene, dibenzylbutane, dibenzylbutyrolactone, dibenzylbutyrolactol, furan, and furofuran types. Within the Meliaceae family, a total of 12 aryltetralin-type lignans, 4 dibenzylbutane-type lignans, 4 furan-type lignans, and 8 furofuran-type lignans have been identified.

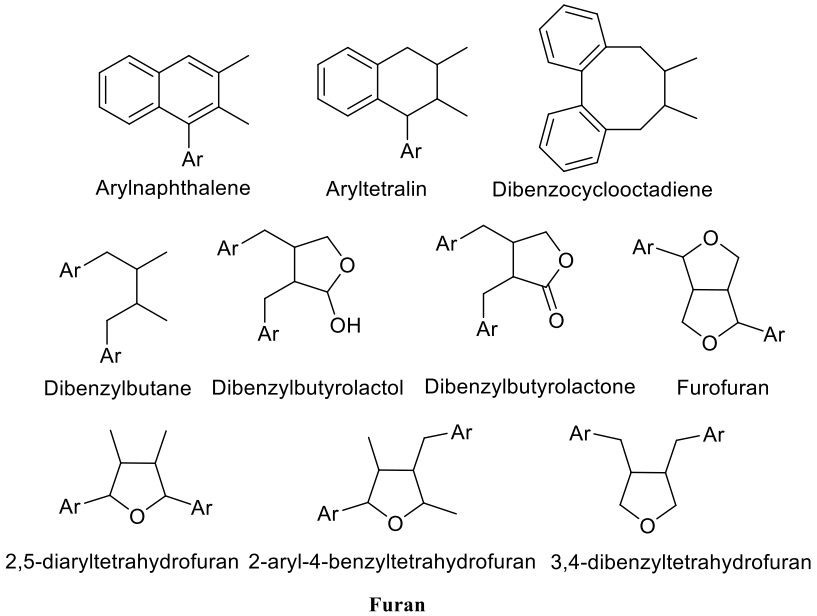

Figure 4 Subtypes of classical lignans (Ar = aryl).

Aryltetralin-type lignans are structurally defined by a tetralin core, consisting of a cyclohexene ring fused to an aromatic ring, which originates from the cyclization of 2 phenylpropanoid units. Within the Meliaceae family, these compounds predominantly occur as glycosides, featuring various substituents such as hydroxyl, methoxy, and monosaccharide units at specific carbon positions. Polystachyol (80), isolated from the bark of *Aphanamixis polystachya* [26], is a non-glycosylated aryltetralin lignan characterized by typical aromatic substitution. From the leaves of *Aglaia odorata*, (−)-isolarisiresinol 3α-*O*-β-D-glucopyranoside (81) [9] has been identified, bearing a glucose moiety linked via a β-glycosidic bond at the 3α position and

defined stereochemistry at its chiral centers. Similarly, (−)-lyoniresinol 3α-*O*-β-D-glucopyranoside (82) [9], isolated from the leaves and twigs of *Walsura robusta*, consists of a lyoniresinol core conjugated to glucose at the same position.

The bark of *Aphanamixis polystachya* also yielded 2 other glycosylated lyoniresinol derivatives, nudiposide (83) and lyoniside (84) [26], each differing in their sugar identities and linkage positions. Additional aryltetralin lignans were found in *Trichilia estipulata*, including (−)-isolariciresinol-3-*O*-β-D-xylopyranoside (85) and (−)-lyoniresinol-3-*O*-β-D-xylopyranoside (86) [42], which are xylose-conjugated derivatives of isolariciresinol and lyoniresinol, respectively. From the same species, a partially methylated analog, (+)-4′-*O*-methyl-9′-deoxiisolariciresinol-3-*O*-β-D-glucopyranoside (87), and a rhamnose conjugate, (−)-lyoniresinol-3-*O*-L-rhamnopyranoside (88) [42], were also identified.

Entanutilin V (89), found in the stem bark of *Entandrophragma utile* [68], possesses a highly substituted aryltetralin skeleton with dense methoxy patterns. From the bark of *Aglaia eximia*, (–)-5′,6-dimethoxyisolariciresinol-(3′,4″-dimethoxy)-3α-*O*-β-D-glucopyranoside (90) was reported [43], featuring 4 methoxy groups and a glucose residue linked at C-3α. The (+)-enantiomer of lyoniresinol, (+)-lyoniresinol 3α-*O*-β-D-glucopyranoside (91), has also been described from *Walsura robusta* [41], in contrast to its (−)-enantiomeric counterpart. (+)-Isolarisiresinol 3α-*O*-β-D-glucopyranoside (92) was found in *Aglaia odorata* [9], while secoisolariciresinol dimethyl ether (93), a dimethylated lignan, was identified from the leaves of *Aglaia testicularis* [44], featuring methoxy substitutions on the aromatic rings. Collectively, these aryltetralin lignans demonstrate extensive structural variation in terms of aromatic substitution, glycosylation patterns, and stereochemistry.

Dibenzylbutane-type lignans are reduced derivatives of pinoresinol, characterized by a saturated butane chain connecting 2 aromatic rings via positions C7 and C7′. These structures typically exist as aglycones or acetylated derivatives. One representative example is (−)-secoisolariciresinol (94), isolated from the fruits of *Melia toosendan* [11]. It contains 2 guaiacyl units linked by a central butane backbone, with hydroxyl groups at both benzylic positions and methoxy substituents on the aromatic rings, typically at C3 and/or C4. Two additional lignans from the bark of *Aglaia elaeagnoidea* are trans-3,4-bis(3,4,5-trimethoxybenzyl)tetrahydrofuran (95) and trans-2,3-bis(3,4,5-trimethoxybenzyl)-1,4-butanediol diacetate (96) [45]. Compound 95 features a cyclic ether (tetrahydrofuran) bridge connecting 2 identically substituted aromatic moieties bearing trimethoxy patterns. In contrast, compound 96 is a linear dibenzylbutane derivative with a central dihydroxybutane unit acetylated at both ends, forming a symmetrical diacetate. These compounds illustrate structural modifications of the dibenzylbutane scaffold via methylation and esterification while maintaining high aromatic substitution symmetry.

Furan-type lignans are characterized by a 5-membered furan ring connecting 2 aromatic moieties via ether and saturated carbon bridges, typically involving C7-*O*-C′ and C8-C′ linkages. (2*R**,3*R**,4*S**)-2,3-Diguaiacyl-4-hydroxy tetrahydrofuran (99), isolated from the fruits of *Melia toosendan* [11], features a symmetrical structure composed of 2 guaiacyl units joined through a central tetrahydrofuran ring. Vladinol D (100), also obtained from *Melia toosendan* [11], presents a furan lignan scaffold with specific hydroxy and methoxy substituents arranged on the aromatic rings. Its structure displays a C-*O*-C linkage between aromatic moieties with a tetrahydrofuran ring as the central connector. The compound (7*S*,8*R*,8′*S*)-3,3′-dimethoxy-4,4′,9-trihydroxy-7,9′-epoxylignan-7′-one (101) [11] contains an epoxy bridge connecting C7 and C9′, forming a 3-membered oxirane ring within the lignan framework. It features methoxy groups at positions 3 and 3′, hydroxy groups at positions 4, 4′, and 9, and a ketone functionality at C7′. The compound's stereochemical complexity exemplifies a furan-type lignan with intricately linked aromatic and saturated systems.

Furofuran-type lignans are distinguished by a bis-tetrahydrofuran system, where 2 guaiacyl or other aromatic units are connected through 2 fused 5-membered oxygen-containing rings, forming a symmetrical framework centered on stereogenic positions at C7, C8, C7′, and C8′. Compounds 5′-demethoxybuddlenol E (102) and buddlenol E (103), both isolated from the fruits of *Melia toosendan* [11], share this structural core but differ by the presence or

absence of a methoxy group at position 5′. Both maintain the characteristic furofuran ring system with hydroxyl and methoxy groups arranged at specific aromatic positions. Ficusesquilignans A (104), also from *Melia toosendan* [11], features a similar backbone but exhibits a more complex pattern of aromatic substitution, representing a highly decorated example within this lignan subclass. (+)-Pinoresinol (105) is a classical furofuran lignan bearing defined stereochemistry at C7, C8, C7′, and C8′, with 2 hydroxyl groups emerging from the aliphatic side. In this context, it is derived from *Melia toosendan* fruit [11]. Yangambin (106), obtained from the leaves of *Aglaia andamanica* [36], is a fully substituted furofuran lignan incorporating methoxy and hydroxyl groups on the aromatic rings, while retaining the typical symmetrical and stereochemically defined furofuran core. These 5 compounds collectively illustrate the structural diversity within the furofuran-type lignans, particularly in terms of aromatic substitution and ring conformation.

Meanwhile, norfurofuran-type lignans represent demethylated and/or structurally simplified versions of the classical furofuran scaffold, distinguished by the loss of one or both 5-membered oxygen-containing rings typical of furofuran lignans. Forsythoside A (97), although traditionally grouped as a phenylpropanoid glycoside, is structurally related to norfurofuran lignans due to its phenylpropanoid linkage and glycosylation pattern, which resemble partial lignan biosynthetic intermediates. This compound was isolated from the leaves of *Aglaia odorata* [9]. Caruilignan C (98), also obtained from *Aglaia odorata* [9], features a lignan backbone with the absence or modification of 1 cyclic ether unit, making it a representative norfurofuran lignan with organized aromatic substitution patterns.

Neolignans are formed through the coupling of 2 phenylpropanoid units at non-C8–C8′ positions, such as C8–C3′, C8–*O*–C′, or C5–C1′, resulting in asymmetrical frameworks and a high degree of structural variability. These compounds differ significantly from classical lignans in terms of connectivity and substitution [40]. Ficusal (107), isolated from *Melia toosendan* fruits [11], is a representative neolignan featuring a flexible carbon backbone without the cyclic saturated systems found in furan or furofuran lignans. It contains 2 guaiacyl-type aromatic rings connected through an aliphatic carbon chain. Dehydrodiconiferyl alcohol-4-β-D-glucoside (108), obtained from the leaves of *Guarea macrophylla* [37], is a glucosylated derivative of dehydrodiconiferyl alcohol, bearing a glucose moiety linked via a β-glycosidic bond at the terminal hydroxyl group.

Erythro-dihydroxydehydrodiconiferyl alcohol (109), from *Melia toosendan* fruits [11], exhibits an erythro configuration at its stereogenic centers, with 2 hydroxyl groups along the connecting carbon chain. Meliasendanin B (110), C (111), and D (112), also from *Melia toosendan* [15], possess more complex neolignan frameworks incorporating methoxy and hydroxyl substituents on both aromatic rings. Their structures are characterized by C–C linked aromatic units and variably hydroxylated or ketone-containing side chains. Compound 1-(4-hydroxy-3-methoxyphenyl)-2-{3-[(1*E*)-3-hydroxy-1-propenyl]-5-methoxyphenoxy}-(1*S*,2*R*)-1,3-propanediol (113), isolated from *Melia toosendan* [15], features a connection between 2 aromatic units through an ether bridge and central aliphatic diol system. The (1*S*,2*R*) configuration on the propane-1,3-diol core adds to its stereochemical uniqueness. Lastly, threo-guaiacylglycerol-β-*O*-4′-coniferyl ether (114) contains guaiacyl and coniferyl groups connected via a β-*O*-4′ ether bond, with the threo configuration common in asymmetrically coupled lignan derivatives.

Following the previous group of neolignans characterized by linear frameworks and inter-unit ether linkages, a subset of compounds from the genus *Aglaia* demonstrates intramolecular coupling that forms heterocyclic ring systems, giving rise to the benzofuran-type neolignans. This subclass is defined by a benzofuran ring formed through internal connection between a phenolic group and an adjacent propenyl chain, resulting in an integrated aromatic cyclic scaffold. Methyl rocaglate (124), also known as aglafolin, isolated from the stems of *Aglaia elliptica* [46], is the foundational compound in this group, featuring methoxy and methyl substituents on the benzofuran core and a fused lactone ring. From the same species, 4′-demethoxy-3′,4′-methylenedioxy-methyl rocaglate (125) replaces 2 hydroxyl groups with a methylenedioxy bridge and lacks the methoxy group at position 4′. Compound 4′-demethoxyrocaglate (126) represents a simpler analog with minimal substitution at key aromatic positions [46]. A more structurally modified derivative, listed as 1-*O*-formyl-4′-

ethylrocaglate (127), incorporates both a formyl and an ethyl group, which are uncommon within the benzofuran framework. Finally, 1-*O*-formyl-4′-demethoxy-3′,4′-methylenedioxy-methyl rocaglate (128) combines all 3 substituent types—formyl, demethoxy, and methylenedioxy—rendering it the most complex member of the series. The aromatic substitution patterns and the presence of fused lactone rings are defining features of this group, indicative of highly specialized secondary metabolism in *Aglaia* species.

Following the discussion of benzofuran-type neolignans with intramolecular aromatic cyclization, the next group, sesquilignans, expands the structural complexity by incorporating 3 phenylpropanoid units. This results in extended carbon frameworks with denser substitution and non-symmetric molecular topologies. *Trans*-2-guaiacyl-3-hydroxymethyl-5-(*cis*-3′-hydroxymethyl-5′-formyl-7′-methoxybenzofuranyl)-7-methoxybenzofuran (129), isolated from the fruits of *Melia toosendan* [11], consists of 2 interconnected benzofuran rings joined via an additional guaiacyl moiety, forming a complex sesquilignan architecture rich in methoxy, formyl, and hydroxymethyl substitutions. This composition reflects biosynthetic elaboration along the phenylpropanoid pathway, with unusual furanic branching not typically found in conventional lignans. Picrasmalignan A (130), also from *Melia toosendan* [11], presents 3 aromatic units linked *via* a multi-branched saturated carbon framework, showing a typical sesquilignan fusion pattern without forming heterocyclic rings. Its core skeleton involves a combination of C–C and C–*O* linkages connecting the aromatic components. The last compound in this group, erythro-guaiacylglycerol-β-*O*-4′-(+)-5,5′-dimethoxylariciresinol ether (131), features a *β*-*O*-4′ linkage between a dimethoxylated lariciresinol unit and a guaiacylglycerol moiety. The erythro configuration on the glycerol chain imparts specific stereochemical identity and adds further structural diversity to this sesquilignan subclass.

Moving from the structurally complex and branched sesquilignans, norlignans offer a more concise yet distinctive framework, characterized by the loss of 1 carbon unit from the typical lignan backbone—hence the prefix “nor”. These structures often involve benzofuran rings or simple ether linkages, accompanied by characteristic aromatic substitution patterns. Cedralin A (132), isolated from the leaves of *Cedrela sinensis* [11], features a substituted benzofuran scaffold with hydroxymethyl and carboxylic acid groups at its side chain, and a (2*S*,3*R*) configuration. It also includes methoxy and methylenedioxy substituents, which are commonly observed in Meliaceae-derived lignans. Rosalaevins A (133), from *Melia toosendan* [11], shares a similar fused aromatic core, although it shows more structural variation in its side chain and ring system. Cedralin B (134), also from *Cedrela sinensis* [47], is a glycosylated and methyl-esterified derivative of Cedralin A. It features a glucose moiety at the hydroxymethyl position and a methyl ester at the carboxyl terminus, distinguishing it from its aglycone counterpart. Meanwhile, erythro-guaiacylglycerol-8′-vanillin ether (135) and threo-guaiacylglycerol-8′-vanillin ether (136), both isolated from *Melia toosendan* [15], represent simpler norlignan structures formed via ether linkage between guaiacyl and vanillin units. Their erythro (135) and threo (136) configurations reflect differences in the spatial orientation of substituents, although their carbon frameworks remain identical.

Continuing from the norlignans bearing vanillin-type terminal groups, the next set of compounds shows further variation in aromatic side chains and glycerol stereochemistry. (2*S*)-3,3-Diguaiacyl-1,2-propanediol (137), isolated from *Melia toosendan* fruits [11], features 2 guaiacyl moieties symmetrically attached at position 3 of the propanediol backbone, forming a saturated, highly symmetric molecule with a single stereocenter at C-2 in the (2*S*) configuration. Erythro-guaiacylglycerol-8′-(4-hydroxymethyl-2-methoxyphenyl) ether (138) and threo-guaiacylglycerol-8′-(4-hydroxymethyl-2-methoxyphenyl) ether (139), also from *Melia toosendan* [15], are linked via an ether bond between guaiacyl and hydroxymethyl-substituted aromatic rings at the 8′ position. The key difference lies in their stereochemistry, erythro versus threo, affecting the spatial relationship of their substituents. The final 2 norlignans, evofolin-B (140) and Meliasendanin A (141), exhibit more elaborate structures combining aromatic and aliphatic systems through flexible saturated carbon chains. Evofolin-B displays symmetrical hydroxymethyl and methoxy substitutions on its aromatic core, while Meliasendanin A features a

linear carbon backbone with multiple aromatic oxygenated functionalities. Both were isolated from *Melia toosendan* fruits [15] and represent characteristic guaiacyl-based norlignans.

Concluding the structural diversity of lignans within the Meliaceae family, several compounds are categorized as "other-type" lignans due to their deviation from classical structural types such as furan, furofuran, neolignan, or norlignan. These compounds, primarily isolated from the bark of *Trichilia catigua* [38], Cinchonain Ic (142) and Id (143) are aromatic oligomers featuring 2 aromatic units linked via saturated carbon bridges, with hydroxyl and ketone substitutions at unusual positions. Catiguanins A (144) and B (145) are structurally related to cinchonains but differ in their aromatic functional group patterns and the number of oxygenated substituents on each ring. Cinchonain Ia (146) and Ib (147) preserve the general oligolignan architecture, with aromatic cores connected either directly or through short aliphatic units, while varying in the position of hydroxyl and carbonyl groups on both saturated and aromatic carbons. Although included within the lignan family, these structures depart significantly from classical lignan definitions, suggesting specialized or divergent biosynthetic pathways within *Trichilia catigua*.

Pharmacological activity

Plants of the Meliaceae family have been traditionally used for decades to treat various conditions, including wounds, headaches, asthma, fever, and dysmenorrhea. Extracts from different plant parts, such as leaves, roots, or fruits, are typically prepared and administered according to the specific condition being treated [48]. This study focuses on the literature related to the pharmacological evaluation of bioactive compounds isolated from various genera within the Meliaceae family.

Antioxidant

A total of 50 compounds from 10 species across 10 genera of the Meliaceae family have been reported to exhibit diverse antioxidant activities (**Table 6**). Simple phenolic compounds, such as (12), displayed moderate antioxidant potency with IC_{50} values ranging from 51.5 to 86.6 μM based on the DPPH assay [41]. Among these, compound (4), a widely known natural antioxidant, exhibited a strong radical-scavenging effect with an SC_{50} of 12.1 ± 0.16 μM [49]. Compounds (10) and (14) also showed notable activities with SC_{50} values of 10.6 ± 0.28 μM and 18.5 ± 0.23 μM, respectively, the latter being isolated from *Toona sinensis* [50]. In comparison, compounds (4) and (10) demonstrated stronger activity within this group, while (12) was categorized as moderately active.

Gallotannin derivatives exhibited superior potency compared to ascorbic acid (SC_{50} = 30.79 μM). The antioxidant capacity increased with the number of galloyl groups, in the order of (13) < (18) < (15) < (16), with respective SC_{50} values of 25.2 ± 0.34, 17.7 ± 0.15, 10.3 ± 0.19, and 7.1 ± 0.26 μM [25]. This trend indicates that additional galloyl groups substantially enhance radical-scavenging potential. Notably, compounds (142) and (143) exhibited the strongest activities with IC_{50} values of 2.5 and 2.3 μM, outperforming other active compounds such as (144 - 147), which also showed strong activity (IC_{50}: 5.1 - 9.4 μM) [38]. These findings suggest that gallotannin derivatives and hydroxyl-rich phenolic structures serve as promising candidates for natural antioxidant development. Compound (71) also demonstrated therapeutic potential via a radical-scavenging mechanism, with an SC_{50} of 12.3 ± 0.6 μM [51].

Flavonoid glycosides showed a wide range of antioxidant activities. Compounds (53) and (62) exhibited strong radical-scavenging effects with IC_{50} values of 23.26 μM and 40.7 μM, respectively [8,18]. These activities are influenced by the hydroxyl groups on ring B, particularly in an ortho (catechol) configuration, as well as the type and number of sugars attached at the C-3 position of the aglycone activities. (54) showed good DPPH activity (IC_{50} = 39.7) but was less active in the superoxide (IC_{50} = 2029 μM) and ABTS (IC_{50} = 513 μM) assays and in inhibiting AGEs formation (IC_{50} = 1246.6 μM) [8]. (50) demonstrated moderate rAR inhibition (46.35% at 22.3 μM) and weak $ABTS^+$ radical scavenging activity (20.74% at 74.3 μM) [52]. (69) demonstrated DPPH (IC_{50} = 41.18 μM), superoxide (IC_{50} = 691.24 μM), ABTS (IC_{50} = 432.02 μM), and AGEs (IC_{50} = 715.54 μM) activities. (57) showed DPPH (IC_{50} = 26.73 μM), superoxide (IC_{50} = 553.6 μM), ABTS (IC_{50} = 270.1 μM), and AGEs (IC_{50} = 775.0 μM) activities. (60) had IC_{50} values of 40.70 μM for DPPH, 928.08 μM for superoxide, 387.60 μM for

ABTS, and 1180.02 μM for AGEs. (52) showed IC_{50} values of 41.35 μM for DPPH, 820.45 μM for superoxide, 366.08 μM for ABTS, and 1193 μM for AGEs. (55) had lower activity with IC_{50} values of 90.1 μM (DPPH), 1075.1 μM (superoxide), 535.3 μM (ABTS), and 1824.3 μM (AGEs). Meanwhile, (58), (59), and (61) had SC_{50} values of 116.64, 103.85, and 287.75 μM, respectively. Structurally, the presence of hydroxyl groups on ring B, particularly in the ortho (catechol) configuration, and the type and number of sugars attached at the C-3 position of the aglycone, greatly contribute to antioxidant activity. Quercetin derivatives tend to be more active than kaempferol due to an additional hydroxyl group at position 3′, which enhances hydrogen donation and free radical stabilization [8,25]. (84) from *A. polystachya* showed strong antioxidant activity with an IC_{50} of 41.6 μM [53]. Other lignan derivatives such as (133) showed strong free radical scavenging capacity in the DPPH assay (SC_{50} = 20.8 μM), comparable to ascorbic acid (SC_{50} = 22.2 μM), moderate reducing activity in the FRAP assay (81.4 μM Trolox/g), and relatively low antioxidant activity in the β-carotene-linoleate model (12.6%) [48]. (103) exhibited excellent DPPH activity with an SC_{50} of 11.2 μM, close to gallic acid (SC_{50} = 10.7 μM) [49]. (123) showed protective effects against H_2O_2-induced oxidative stress in H9c2 cells, increasing cell viability to 82.61 ± 1.87% at 200 μM [56]. (117) inhibited NO production in LPS-stimulated BV-2 cells with an IC_{50} of 17.8 ± 0.9 μM, stronger than L-NMMA (IC_{50} = 22.7 ± 1.1 μM), while maintaining high cell viability (99.7 ± 6.1% at 50 μM), indicating non-toxic behavior. In contrast, (118) exhibited moderate activity (IC_{50} = 31.4 ± 1.3 μM) but remained safe (cell viability = 94.1 ± 3.6%) [57]. (100) showed high activity against DPPH (IC_{50} = 7.3 μM) and ABTS (IC_{50} = 11.3 μM) radicals [58]. (94) demonstrated very strong antioxidant potential, reducing PMNL chemiluminescence (CL) by 91.2% at 2.5 mg/mL, 4.86 times more potent than vitamin E and 3.82 times stronger than its parent compound, SDG. SAR studies revealed that free phenolic groups and conjugated aromatic systems enhance radical-scavenging activity, while stereochemical isomerism (e.g., threo- vs. erythro-) and hydroxyl/methoxyl substituents on guaiacyl and coniferyl units affect NO inhibition and cytotoxicity. Additionally, the compound's ability to stabilize free radicals or chelate metals contributes to overall antioxidant efficacy [59]. (110 - 112, 141) exhibited varying scavenging activity, with IC_{50} values indicating good antioxidant potential. (141) showed the strongest activity among them (IC_{50} = 62.8 μM), though weaker than ascorbic acid, but still more effective than the others in the group. (110) had an IC_{50} of 111.2 μM, showing decent antioxidant potential. (111) exhibited relatively strong activity (IC_{50} = 81.9 μM), and (112) had an IC_{50} of 89.1 μM, still within a moderate range. Structurally, hydroxyl group presence and potential conjugated systems in the limonoid scaffold influence ABTS scavenging efficacy, where specific functional group substitutions can significantly enhance or reduce activity [15].

Complex compound (113) showed lower scavenging activity than the others, with an IC_{50} of 200.9 μM. The weakest activity was observed in (114) (IC_{50} = 267.4 μM against ABTS radicals). Moderate activity was seen in (135) (IC_{50} = 126.2 μM), (136) (IC_{50} = 117.6 μM), (138) (IC_{50} = 125.8 μM), and (139) (IC_{50} = 104.4 μM). Conversely, (105) exhibited very strong ABTS activity (IC_{50} = 45.1 μM), close to the potency of ascorbic acid. (140) had good scavenging activity (IC_{50} = 125.0 μM), although lower than more active compounds. (101) showed moderate activity with an IC_{50} of 130.8 μM [15]. (91) exhibited antioxidant activity in the DPPH assay (IC_{50} = 68.7 μM) and very strong superoxide scavenging (IC_{50} = 0.8 mM). (132) showed stronger antioxidant activity than (82), with an IC_{50} of 51.5 μM, hydroxyl radical scavenging activity of 7.4 μM, and very strong superoxide scavenging (IC_{50} = 0.7 mM) [41]. Finally, the flavonoid compound (34) exhibited very high antioxidant activity as a free radical scavenger, even surpassing vitamin C. It had an SC_{50} of 29.7 μM and showed 83.11% inhibition at a concentration of 54.2 μM. This high activity is associated with the presence of ortho-dihydroxy (catechol) groups on the B ring, which contribute to hydrogen atom donation for neutralizing free radicals, making (34) one of the most effective antioxidants in this group [54].

Table 1 Simple phenolic compounds from Meliaceae family.

	Compound	Species	Part	Extract	References
1	4-hydroxybenzoic acid	*Trichilia heudelotti*	Leaves	EtOAc	[17]
2	Vanillic acid	*Chisocheton penduliflorus*	Wood and leaves	$CHCl_3$	[22]
3	4-hydroxy-3,5-dimethylbenzoic acid	*Ekebergia senegalensis A.*	Stem barks	CH_2Cl_2/MeOH	[21]
4	Gallic acid	*Toona sinensis*	Leaves and shoots	EtOAc	[25]
5	Protocatechuic acid	*Trichilia heudelotti*	Leaves	EtOAc	[17]
6	2-methylproto-catechuic acid	*Trichilia heudelotti*	Leaves	EtOAc	[17]
7	Atraric acid	*Ekebergia capensis*	Barks	*n*-hexane	[23]
8	(*E*)-4-hydroxycinnamic acid	*Xylocarpus granatum*	Seeds	EtOAc	[24]
9	2-propionoxy-b-resorcylic acid	*Trichilia heudelotti*	Leaves	EtOAc	[17]
10	Trigallic acid	*Toona sinensis*	Leaves and shoots	EtOAc	[25]
11	Senegalin	*Ekebergia senegalensis A.*	Stem barks	CH_2Cl_2/MeOH (1:1)	[21]
12	3,4,5-trimethoxyphenyl β-D-glucopyranoside	*Walsura robusta Roxb.*	Leaves and twigs	MeOH	[41]
13	6-*O*-galloyl-D-glucose	*Toona sinensis*	Leaves and shoots	EtOAc	[25]
14	Methyl gallate	*Toona sinensis*	Leaves and shoots	EtOAc	[25]
15	1,2,3,6-tetra-*O*-galloyl-β-D-glucopyranose	*Toona sinensis*	Leaves and shoots	EtOAc	[25]
16	1,2,3, 4,6-penta-*O*-galloyl-β-D-glucopyranose	*Toona sinensis*	Leaves and shoots	EtOAc	[25]
17	(+)-Ent-ficusol	*Aglaia odorata Lour.*	Leaves	EtOAc	[9]
18	1,2,3-tri-*O*-galloyl-β-D-glucopyranose	*Toona sinensis*	Leaves and shoots	EtOAc	[25]

Table 2 Coumarin compounds from Meliaceae family.

	Compound	Species	Part	Extract	References
19	Scopoletin	*Guarea rhophalocarpa*	Leaves	$CHCl_3$	[28]
20	4,6-dimethoxy-5-methylcoumarin	*Ekebergia senegalensis A.*	Stem barks	CH_2Cl_2/MeOH (1:1)	[21]
21	6-hydroxy-4-methoxy-5-methylcoumarin	*Ekebergia senegalensis*	Stem barks	CH_2Cl_2/MeOH (1:1)	[21]
22	5-(hydroxymethyl)4-methoxycoumarin	*Ekebergia senegalensis A.*	Stem barks	CH_2Cl_2/MeOH (1:1)	[21]
23	Scoparone	*Chisocheton penduliflorus*	Wood and leaves	$CHCl_3$	[22]
24	4-methoxy-5-methylcoumarin	*Ekebergia capensis and Ekebergia senegalensis*	Barks	*n*-hexane	[23]
25	Ekersenin (pereflorin)	*Ekebergia capensis*	Stem barks	EtOAc	[73]

	Compound	Species	Part	Extract	References
26	5-(4-hydroxyphenethenyl)-4,7-dimethoxycoumarin	*Ekebergia benguelensis*	Roots barks	MeOH	[30]
27	3,4-dihydro-4,4,5,8-tetramethylcoumarin	*Azadirachta indica A. Juss.*	Fruits	EtOH	[29]
28	3,4-dihydro-4,4,7,8-tetramethylcoumarin-6-ol	*Azadirachta indica A. Juss.*	Fruits	EtOH	[29]

Table 3 Stilbene compounds from Meliaceae family.

	Compound	Species	Part	Extract	References
29	5-[(1*E*)-2-(4-hydroxyphenyl)ethenyl]-4,7-dimethoxy-3-methyl-2H-1-benzopyran-2-one	*Ekebergia benguelensis*	Roots barks	MeOH	[30]
30	5-[(1*E*)-2-(4-D-glucopyranosyloxyphenyl)ethenyl]-4,7-dimethoxy-3-methyl-2H-1-benzopyran-2-one	*Ekebergia benguelensis*	Roots barks	MeOH	[30]
31	1-{2-hydroxy-6-[(1*E*)-2-(4-hydroxyphenyl)ethenyl]-4-methoxyphenyl}-2- methyl-1-propanone	*Ekebergia benguelensis*	Roots barks	MeOH	[30]
32	1-{2,4-dihydroxy-6-[(1*E*)-2-(4-hydroxyphenyl)ethenyl]-phenyl}-2-methyl-1-propanone	*Ekebergia benguelensis*	Roots barks	MeOH	[30]

Tabel 4 Flavonoid compounds from Meliaceae family.

	Compound	Species	Part	Extract	References
33	Catechin	*Swietenia mahagoni (L.) Jacq.*	Leaves	n-BuOH	[31]
34	3,4′,5,7-tetrahydroxyflavanone	*Xylocarpus granatum*	Seeds	EtOAc	[24]
35	Euchrestaflavanone A	*Azadirachta indica var. siamensis*	Flowers	MeOH	[32]
36	4′-*O*-methyllespedezaflavanone C	*Azadirachta indica var. siamensis*	Flowers	MeOH	[32]
37	3′-(3-hydroxy-3 methylbutyl) naringenin	*Azadirachta indica var. siamensis*	Flowers	MeOH	[32]
38	8-prenylnaringenin	*Azadirachta indica var. siamensis*	Flowers	MeOH	[32]
39	4'-*O*-methyl-8-prenylnaringenin	*Azadirachta indica var. siamensis*	Flowers	MeOH	[32]
40	3'-prenylnaringenin	*Azadirachta indica var. siamensis*	Flowers	MeOH	[32]
41	Kaempferol	*Aglaia eximia*	Barks	EtOAc	[33]
42	Quercetin	*Pseudocedrela kotschyi (Schweinf.)*	Roots	MeOH	[34]
43	8-C-methyl quercetin	*Amoora Rohituka*	Roots	MeOH	[35]
44	8-C-methyl-quercetin-5,7,3',4'-tetramethyl ether	*Amoora Rohituka*	Roots	MeOH	[35]
45	3,4′,7-trimethyl esther	*Pseudocedrela kotschyi (Schweinf.)*	Roots	MeOH	[34]
46	Kaempferide	*Azadirachta indica var. siamensis,*	Flowers	MeOH	[32]
47	3-*O*-methyl mearnsetin	*Azadirachta indica var. siamensis,*	Flowers	MeOH	[32]
48	3,6,8-trihydroxy-2-(3,4-dihydroxylphenyl)-4H-chrom-4-one	*Pseudocedrela kotschyi (Schweinf.)*	Roots	MeOH	[34]

	Compound	Species	Part	Extract	References
49	3-methoxy-3'-prenylkaempferol	*Azadirachta indica var. siamensis,*	Flowers	MeOH	[32]
50	Kaempferol-3-*O*-β-D-glucopyranoside	*Aglaia andamanica*	Leaves	MeOH	[36]
51	Kaempferol 7-*O*-β-D-glucopyranoside	*Guarea macrophylla*	Leaves	*n*-BuOH	[37]
52	Quercetin-3-*O*-α-rhamnoside	*Cedrela serrata*	Leaves	EtOAc	[8]
53	Quercetin-3-*O*-β-D-glucopyranoside	*Cedrela serrata*	Leaves	EtOAc	[8]
54	Kaempferol-3-*O*-β-galactoside	*Cedrela serrata*	Leaves	EtOAc	[8]
55	Kaempferol-3-*O*-β-glucoside	*Cedrela serrata*	Leaves	EtOAc	[8]
56	Quercetin-3-*O*-glucoside	*Swietenia mahagoni (L.) Jacq.*	leaf	*n*-BuOH	[31]
57	Kaempferol-3-*O*-glucosyl (1→2) rutinoside	*Cedrela serrata*	Leaves	EtOAc	[8]
58	Quercetin-3-*O*-α-L-rhamnopyranoside	*Toona sinensis*	Leaves and shoots	EtOAc	[25]
59	Rutin	*Toona sinensis*	Leaves and shoots	EtOAc	[25]
60	Quercetin-3-*O*-β-galactoside	*Cedrela serrata*	Leaves	EtOAc	[17]
61	Kaempferol-3-*O*-L-arabinopyranoside	*Toona sinensis*	Leaves and shoots	EtOAc	[25]
62	Quercetin-3-*O*-β-D-galactopyranoside	*Guarea macrophylla*	Leaves	n-BuOH	[37]
63	Kaempferol 3-*O*-rhamnoside	*Melia azedarach*	Leaves	EtOH	[27]
64	Kaempferol 3-*O*-rutinoside	*Melia azedarach*	Leaves	EtOH	[27]
65	Quercetin-3-*O*-rutinoside	*Melia azedarach*	Leaves	EtOH	[27]
66	Kaempferol-3-*O*-α-L-rhamnoside	*Aglaia eximia*	Barks	EtOAc	[33]
67	Kaempferol-3-*O*-β-D-glucosyl-α-L-rhamnoside	*Aglaia eximia*	Barks	EtOAc	[33]
68	Quercetin-3-*O*-[rhamnosyl 1→6(4″-lactoyl glucoside)]-4′-O-glucoside	*Melia azedarach*	Leaves	EtOH	[27]
69	Kaempferol-3-*O*-rhamnosyl (1→6)-(4″-trans-p-coumaroyl)-galactoside	*Cedrela serrata*	Leaves	EtOAc	[8]
70	5-hydroxy-3,4′,7,-trimethoxyflavone	*Aglaia andamanica*	Leaves	MeOH	[36]
71	Retusin	*Aglaia andamanica*	Leaves	MeOH	[36]
72	Pachypodol	*Aglaia andamanica*	Leaves	MeOH	[36]
73	Chrysin	*Amoora cucullata*	Leaves	EtOAc	[20]
74	Apigenin	*Amoora cucullata*	Leaves	EtOAc	[20]
75	8-C-methyl-5,7,3′,4′-tetrahydroxyflavone-3-*O*-β-D-xylopyranosid	*Amoora Rohituka*	Roots	MeOH	[25]
76	Robustaflavone 4′,7″-dimethyl ether	*Dysoxylum lenticellare gillespie*	Leaves	MeOH	[39]

	Compound	Species	Part	Extract	References
77	Aglaodoratas A	*Aglaia odorata Lour.*	Leaves	EtOAc	[9]
78	Aglaodoratas B	*Aglaia odorata Lour.*	Leaves	EtOAc	[9]
79	Aglaodoratas C	*Aglaia odorata Lour.*	Leaves	EtOAc	[9]

Table 5 Lignan compounds from Meliaceae family.

	Compound	Species	Part	Extract	References
80	Polystachyol	*Aphanamixis polystachya*	Barks	*n*-BuOH	[26]
81	(−)-isolarisiresinol 3α-*O*-β-D-glucopyranoside	*Aglaia odorata Lour.*	Leaves	EtOAc	[9]
82	(−)-Lyoniresinol 3α-*O*-β-D-glucopyranoside	*Walsura robusta Roxb.*	Leaves and twigs	*n*-BuOH	[41]
83	Nudiposide	*Aphanamixis polystachya*	Barks	*n*-BuOH	[26]
84	Lyoniside	*Aphanamixis polystachya*	Barks	*n*-BuOH	[26]
85	(-)-isolariciresinol-3-*O*-D-xylopyranoside	*Trichilia estipulata*	Barks	MeOH	[42]
86	(-)-lyoniresinol-3-*O*-D-xylopyranosid	*Trichilia estipulata*	Barks	MeOH	[42]
87	(+)-4′-0-methyl-9′-deoxiisolariciresinol-3-*O*-D-glucopyranoside	*Trichilia estipulata*	Barks	MeOH	[42]
88	(-)-lyoniresinol-3-L-rhamnopyranosid	*Trichilia estipulata*	Barks	MeOH	[42]
89	Entanutilin V	*Entandrophragma utile*	Stem barks	CH_2Cl_2	[68]
90	(–)-5′,6-dimethoxyisolariciresinol-(3′,4″-dimethoxy)-3α-*O*-β-dglucopyranoside	*Aglaia eximia*	Barks	MeOH	[43]
91	(+)-Lyoniresinol 3α-*O*-D-glucopyranoside	*Walsura robusta Roxb.*	Leaves and twigs	*n*-BuOH	[41]
92	(+)-isolarisiresinol 3α-*O*-β-D-glucopyranoside	*Aglaia odorata Lour.*	Leaves	MeOH	[9]
93	Secoisolariciresinol dimethyl ether	*Aglaia testicularis*	Leaves	EtOAc	[44]
94	(−)-secoisolariciresinol	*Melia toosendan*	Fruits	EtOH	[11]
95	Trans - 3,4 - Bis(3,4,5 trimethoxybenzyl)tetrahydrofuran	*Aglaia elaeagnoidea*	Barks	CH_2Cl_2	[45]
96	Trans-2,3-bis(3,4,5-trimethoxybenzyl)-1,4-butanediol diacetate	*Aglaia elaeagnoidea*	Barks	CH_2Cl_3	[45]
97	Forsythoside A	*Aglaia odorata Lour.*	Leaves	MeOH	[9]
98	Caruilignan C	*Aglaia odorata Lour.*	Leaves	MeOH	[9]
99	(2*R*,3*R*,4*S*)-2,3-Diguaiacyl-4-hydroxyl tetrahydrofuran	*Melia toosendan*	Fruits	EtOH	[11]
100	Vladinol D	*Melia toosendan*	Fruits	EtOH	[11]
101	(7*S*,8*R*,8′*S*)-3,3′-dimethoxy-4,4′,9-trihydroxy-7,9′-epoxylignan-7′-one	*Melia toosendan*	Fruits	*n*-BuOH	[15]
102	5′-demethoxybuddlenol E	*Melia toosendan*	Fruits	EtOH	[11]
103	Buddlenol E	*Melia toosendan*	Fruits	EtOH	[11]

	Compound	Species	Part	Extract	References
104	Ficusesquilignans A	*Melia toosendan*	Fruits	EtOH	[11]
105	(+)-pinoresinol	*Melia toosendan*	Fruits	EtOH	[11]
106	Yangambin	*Aglaia andamanica*	Leaves	MeOH	[36]
107	Ficusal	*Melia toosendan*	Fruits	EtOH	[11]
108	Dehydrodiconiferyl alcohol-4-D-glucoside	*Guarea macrophylla*	Leaves	*n*-BuOH	[37]
109	Erythro-dihydroxydehydrodiconiferyl alcohol	*Melia toosendan*	Fruits	EtOH	[11]
110	Meliasendanin B	*Melia toosendan*	Fruits	*n*-BuOH	[15]
111	Meliasendanin C	*Melia toosendan*	Fruits	*n*-BuOH	[15]
112	Meliasendanin D	*Melia toosendan*	Fruits	*n*-BuOH	[15]
113	1-(4-hydroxy-3-methoxyphenyl)-2-{3-[(1*E*)-3-hydroxy-1-propenyl]-5- methoxyphenoxy}-(1*S*, 2*R*)-1,3-propanediol	*Melia toosendan*	Fruits	*n*-BuOH	[15]
114	Threo-guaiacylglycerol-β-*O*-4′-coniferyl ether	*Melia toosendan*	Fruits	*n*-BuOH	[15]
115	Threo-guaiacylglycerol-β-coniferyl aldehyde ether	*Melia toosendan*	Fruits	EtOH	[11]
116	Erythro-guaiacylglycerol-β-coniferyl aldehyde ether	*Melia toosendan*	Fruits	EtOH	[11]
117	Threo-guaiacylglycerol-β-coniferyl ether	*Melia toosendan*	Fruits	EtOH	[11]
118	Erythro-guaiacylglycerol-β-coniferyl ether	*Melia toosendan*	Fruits	EtOH	[11]
119	Threo-Guaiacylethoxyglycerol-β-*O*-4′-coniferyl aldehyde ether	*Melia toosendan*	Fruits	EtOH	[11]
120	Threo-Guaiacylethoxyglycerol-β-*O*-4′-guaiacyl aldehyde ether	*Melia toosendan*	Fruits	EtOH	[11]
121	Erythro-Guaiacylethoxyglycerol-β-*O*-4′-guaiacyl aldehyde ether	*Melia toosendan*	Fruits	EtOH	[11]
122	Erythro-Guaiacylethoxyglycerol-β-*O*-4′-coniferyl aldehyde ether	*Melia toosendan*	Fruits	EtOH	[11]
123	Leptolepisol D	*Melia toosendan*	Fruits	EtOH	[11]
124	Methyl rocaglate	*Aglaia elliptica*	Stems	$CDCl_3$	[46]
125	4′-demethoxy-3′,4′-methylenedioxy-methyl rocaglate	*Aglaia elliptica*	Stems	$CDCl_3$	[46]
126	4′-Demethoxyrocaglate	*Aglaia elliptica*	Stems	$CDCl_3$	[46]
127	1-*O*-formyl-4'-ethylrocaglate	*Aglaia elliptica*	Stems	$CDCl_3$	[46]
128	1-*O*-formyl-4'-demethoxy-3',4'-methylenedioxy-methyl rocaglate	*Aglaia elliptica*	Stems	$CDCl_3$	[46]
129	Trans-2-Guaiacyl-3-hydroxymethyl-5-(*cis*-3′-hydroxymethyl-5′-formyl-7′-methoxybenzofuranyl)-7-methoxybenzofuran	*Melia toosendan*	Fruits	EtOH	[11]

	Compound	Species	Part	Extract	References
130	Picrasmalignan A	*Melia toosendan*	Fruits	EtOH	[11]
131	Erythro-Guaiacylglycerol-β-*O*-4′-(+)-5,5′-dimethoxylariciresinol ether	*Melia toosendan*	Fruits	EtOH	[11]
132	Cedralin A	*Cedrela sinensis A. Juss*	Leaves	AcOEt	[47]
133	Rosalaevins A	*Melia toosendan*	Fruits	EtOH	[11]
134	Cedralin B	*Cedrela sinensis A. Juss*	Leaves	AcOEt	[47]
135	Erythro-guaiacylglycerol-8′-vanillin ether	*Melia toosendan*	Fruits	*n*-BuOH	[15]
136	Threo-guaiacylglycerol 8′-vanillin ether	*Melia toosendan*	Fruits	*n*-BuOH	[15]
137	(2*S*)-3,3-diguaiacyl-1,2-propanediol	*Melia toosendan*	Fruits	EtOH	[11]
138	Erythro-guaiacylglycerol-8′-(4-hydroxymethyl-2-methoxyphenyl) ether	*Melia toosendan*	Fruits	*n*-BuOH	[15]
139	Threo-guaiacylglycerol-8′-(4-hydroxymethyl-2-methoxyphenyl) ether	*Melia toosendan*	Fruits	*n*-BuOH	[15]
140	Evofolin-B	*Melia toosendan*	Fruits	*n*-BuOH	[15]
141	Meliasendanin A	*Melia toosendan*	Fruits	*n*-BuOH	[15]
142	Cinchonain Ic	*Trichilia catigua*	Barks	MeOH	[38]
143	Cinchonain Id	*Trichilia catigua*	Barks	MeOH	[38]
144	Catiguanins A	*Trichilia catigua*	Barks	MeOH	[38]
145	Catiguanins B	*Trichilia catigua*	Barks	MeOH	[38]
146	Cinchonain Ia	*Trichilia catigua*	Barks	MeOH	[38]
147	Cinchonain Ib	*Trichilia catigua*	Barks	MeOH	[38]

Table 6 Antioxidant activity of phenolic compounds.

Species	Part	Compound	Bioactivity result	References
Toona sinensis	Leaves and shoots	Gallic acid (4)	DPPH (SC_{50} 12.1 ± 0.16 μM)	[49]
		Trigallic acid (10)	DPPH (SC_{50} 10.6 ± 0.28 μM)	[25]
Walsura robusta Roxb.	Leaves and twigs	3,4,5-trimethoxyphenyl β-D-glucopyranoside (12)	DPPH (IC_{50} 51.5 – 86.6 μM)	[41]
Toona sinensis	Leaves and shoots	6-*O*-galloyl-D-glucose (13)	DPPH (SC_{50} 25.2 ± 0.34 μM)	[25]
		Methyl gallate (14)	H_2O_2 protection (SC_{50} 18.5 ± 0.23 μM)	[50]
		1,2,3,6-tetra-*O*-galloyl-β-D-glucopyranose (15)	DPPH (SC_{50} 10.3 ± 0.19 μM)	[25]

Species	Part	Compound	Bioactivity result	References
		1,2,3, 4,6-penta-*O*-galloyl-β-D-glucopyranose (16)	DPPH (SC_{50} 7.1 ± 0.26 μM)	[25]
		1,2,3-tri-*O*-galloyl-β-D-glucopyranose (18)	DPPH (SC_{50} 17.7 ± 0.15 μM)	[25]
Xylocarpus granatum	Seeds	3,4′,5,7-tetrahydroxyflavanone (34)	SC_{50} = 29.7 μM; Inhibition = 83.11% @ 188.0 μM	[24]
Aglaia andamanica	Leaves	Kaempferol-3-*O*-β-D-glucopyranoside (50)	rAR inhibition: 46.35% @22.30 μM, $ABTS^{+}$: 20.74% @74.27 μM	[52]
Cedrela serrata	Leaves	Quercetin-3-*O*-α-rhamnoside (52)	DPPH = 41.35 μM; Superoxide = 820.45 μM; ABTS = 366.08 μM; AGEs = 1193 μM	[8]
		Quercetin-3-*O*-β-D-glucopyranoside (53)	DPPH (IC_{50} 23.26 μM)	[8]
		Kaempferol-3-*O*-β-galactoside (54)	DPPH = 39.70 μM; Superoxide = 2029.1 μM; ABTS = 513.1 μM; AGEs = 1246.6 μM	[8]
		Kaempferol-3-*O*-β-glucoside (55)	DPPH = 90.1 μM; Superoxide = 1075.1 μM; ABTS = 535.3 μM; AGEs = 1824.3 μM	[8]
		Kaempferol-3-*O*-glucosyl (1→2) rutinoside (57)	DPPH = 26.73 μM; Superoxide = 553.6 μM; ABTS = 270.1 μM; AGEs = 775.0 μM	[8]
Toona sinensis	Leaves and shoots	Quercetin-3-*O*-α-L-rhamnopyranoside (58)	SC_{50} = 116.64 μM	[25]
		Rutin (59)	SC_{50} = 103.9 μM	[25]
Cedrela serrata	Leaves	Quercetin-3-*O*-β-galactoside (60)	DPPH = 40.7 μM; Superoxide = 927.6 μM; ABTS = 387.5 μM; AGEs = 1,180 μM	[8]
Toona sinensis	Leaves and shoots	Kaempferol-3-*O*-L-arabinopyranoside (61)	SC_{50} = 289.2 ± 5.9 μM	[25]
Guarea macrophylla	Leaves	Quercetin-3-*O*-β-D-galactopyranoside (62)	DPPH, IC_{50} = 40.7 μM	[18]
Cedrela serrata	Leaves	Kaempferol-3-*O*-rhamnosyl (1→6)-(4”-trans-p-coumaroyl)-galactoside (69)	DPPH = 41.18 μM; Superoxide = 691.2 μM; ABTS = 432.0 μM; AGEs = 715.6 μM	[8]
Aglaia andamanica	Leaves	Retusin (71)	Radical scavenging, SC50 = 12.3 ± 0.6 and 11.8 ± 0.8 mm	[51]
Walsura robusta Roxb.	Leaves and twigs	(−)-Lyoniresinol 3α-*O*-β-D-glucopyranoside (82)	DPPH, IC_{50} = 51.5 μM; Hydroxyl = 7.4 μM; Superoxide = 700 μM	[41]
Aphanamixis polystachya	Barks	Lyoniside (84)	DPPH, IC_{50} = 41.6 μM	[53]

Species	Part	Compound	Bioactivity result	References
Walsura robusta Roxb.	Leaves and twigs	(+)-Lyoniresinol 3α-*O*-β-D-glucopyranoside (91)	DPPH, IC_{50} = 68.7 μM; Superoxide = 0.8 mM	[41]
Melia toosendan	Fruits	(−)-secoisolariciresinol (94)	Chemiluminescence inhibition = 91.2% @ 2.5 mg/mL.	[59]
		Vladinol D (100)	DPPH = 7.3 μM; ABTS = 11.3 μM	[58]
		(7*S*,8*R*,8′*S*)-3,3′-dimethoxy-4,4′,9-trihydroxy-7,9′-epoxylignan-7′-one (101)	ABTS, IC_{50} = 130.8 μM	[15]
		Buddlenol E (103)	DPPH, SC_{50} = 11.2 μM	[55]
		(+)-pinoresinol (105)	ABTS, IC_{50} = 45.1 μM	[15]
Melia toosendan	Fruits	Meliasendanin B (110)	ABTS, IC_{50} = 111.2 μM	[15]
		Meliasendanin C (111)	ABTS, IC_{50} = 81.9 μM	[15]
		Meliasendanin D (112)	ABTS, IC_{50} = 89.1 μM	[15]
		1-(4-hydroxy-3-methoxyphenyl)-2-{3-[(1*E*)-3-hydroxy-1-propenyl]-5- methoxyphenoxy}-(1*S*, 2*R*)-1,3-propanediol (113)	ABTS, IC_{50} = 200.9 μM	[15]
		Threo-guaiacylglycerol-β-*O*-4′-coniferyl ether (114)	ABTS, IC_{50} = 267.4 μM	[15]
		Threo-guaiacylglycerol-β-coniferyl ether (117)	NO inhibition: IC_{50} = 17.8 ± 0.9 μM; Cell viability = 99.7%.	[57]
		Erythro-guaiacylglycerol-β-coniferyl ether (118)	IC_{50} = 31.4 ± 1.3 μM; viability = 94.1%	[57]
		Leptolepisol D (123)	H_2O_2 protection, viability = 82.61 ± 1.87% @ 200 μM	[56]
		Rosalaevins A (133)	DPPH (SC_{50} = 20.8 μM), FRAP = 81.4 μM Trolox/g; β-caroten = 12.6%	[54]
		Erythro-guaiacylglycerol-8′-vanillin ether (135)	ABTS (IC_{50} 126.2 μM)	[15]
		Threo-guaiacylglycerol 8′-vanillin ether (136)	ABTS (IC_{50} 117.6 μM)	[15]
		Erythro-guaiacylglycerol-8′-(4-hydroxymethyl-2-methoxyphenyl) ether (138)	ABTS (IC_{50} 125.8 μM)	[15]
		Threo-guaiacylglycerol-8′-(4-hydroxymethyl-2-methoxyphenyl) ether (139)	ABTS (IC_{50} 104.4 μM)	[15]
		Evofolin-B (140)	ABTS (IC_{50} 125.0 μM)	[15]
		Meliasendanin A (141)	ABTS (IC_{50} 62.8 μM)	[15]

Species	Part	Compound	Bioactivity result	References
Trichilia catigua	Barks	Cinchonain Ic (142)	DPPH (IC_{50} 2.5 μM)	[38]
		Cinchonain Id (143)	DPPH (IC_{50} 2.3 μM)	[38]
		Catiguanins A (144)	DPPH (IC_{50} 7.1 μM)	[38]
		Catiguanins B (145)	DPPH (IC_{50} 6.7 μM)	[38]
		Cinchonain Ia (146)	DPPH (IC_{50} 9.4 μM)	[38]
		Cinchonain Ib (147)	DPPH (IC_{50} 5.1 μM)	[38]

Anticancer

A total of 34 phenolic compounds from 10 species across 7 genera in the Meliaceae family have demonstrated a wide spectrum of anticancer activity against various human cancer cell lines (**Table 7**). Among the simple phenolics, (2) was noteworthy for enhancing the sensitivity of both K562 and multidrug-resistant K562/Dox leukemia cells to pirarubicin (Pira), resulting in significantly reduced IC_{50} values at concentrations of 0.01 - 10 mM over 48 - 72 h [19].

Flavonoids also showed diverse biological effects. For instance, (72) protected hepatocytes from oxidative stress via Nrf2 activation (IC_{50} = 185.6 μM, CaCo-2 cells) [54,59]. Flavonols such as (33) and (56) exhibited strong cytotoxicity toward leukemia cell lines (U937, K562, and HL-60) Specifically, (33) showed IC_{50} values of 11.2 μM (U937), 7.1 - 9.1 μM (K562), and 2.34 - 43.5 μM (HL-60), while (56) displayed IC_{50} values of 5.45 μM (U937), 5.68 μM (K562), and 6.6 μM (HL-60), indicating potent antiproliferative activity against hematologic malignancies. By contrast, (37) was inactive. Among flavonoids with broader cytotoxic profiles, (35) and (36) exhibited potent activity against lung (A549), gastric (AZ521), and breast (SK-BR-3) cancer cells, with IC_{50} values in the 6.3 - 9.9 μM range. The methoxylated flavonoid (39) was more active than its unmethylated analog (38), suggesting the influence of methylation on potency. (49) showed the most consistent activity across all tested cell lines, while (41) was active against P-388 leukemia cells (IC_{50} = 4.26 μM), but its glycosylated derivatives (67) and (68) were markedly less potent (IC_{50} = 992.8 to > 2312 μM), indicating a loss of activity due to sugar moieties.

Within the lignan subclass, a number of rocaglate-type compounds displayed nanomolar to sub-nanomolar cytotoxicity. (124) was highly potent (IC_{50} = 0.0023 – 0.068 μM, BC1, HT-1080, Lu1), and (125) exhibited broad-spectrum activity (ZR-75, U373 = 0.0018 – 0.0045 μM). In contrast, (126) and (127) had significantly weaker activity (IC_{50} = 0.45 and 3.18 μM, respectively), while (128) restored high potency (ZR-75 = 0.0023 μM) [46]. Enantiomeric differences also played a role in cytotoxicity, with (115-2b) (IC_{50} = 39.02 μM) being more active than (115-2a) (67.97 μM), and (116-1b) (45.56 μM) more active than (116-1a) (82.66 μM) [78]. Compound (107) displayed moderate cytotoxicity toward Hep3B liver cancer cells (EC_{50} = 258.5 μM) far less potent than the reference drug doxorubicin (EC_{50} = 0.57 μM) [11,74]. Limonoid analogs showed modest activity. (132) demonstrated weak cytotoxicity against HL-60 and K562 (IC_{50} = 76.1 μM and 65.0 μM), and its glycosylated derivative (134) showed negligible activity (IC_{50} > 58 μM) [47].

Coumarin derivatives exhibited a range of activity. Compound (26) showed moderate and selective activity against prostate cancer cells (LNCaP, ED_{50} = 22.84 μM) [30], while (21) was moderately active against oral carcinoma cells (KB, IC_{50} = 23.3 μM) [21,76]. In contrast, (23) showed weak activity against pancreatic cancer cell lines (Capan-2 and SW1990, IC_{50} = 225.2 and 209.1 μM) [22,75]. The stilbene derivative (29) demonstrated moderate cytotoxicity against Lu1 cells (ED_{50} = 15.1 μM), while compound (30) was considered weakly active with ED_{50} values > 40 μM. On the other hand, compounds (31) and (32) displayed moderate and

selective activity against KB and LNCaP cell lines, with ED_{50} values of 31.7 and 25.2 µM, respectively [30].

Table 7 Cytotoxic activity of phenolic compounds.

Spesies	Part	Compound	Bioactivity result	References
Chisocheton penduliflorus	Wood and leaves	Vanillic acid (2)	K562/K562Dox: 0.01 – 10 mM	[19]
Ekebergia senegalensis	Stem barks	6-hydroxy-4- methoxy-5-methylcoumarin (21)	KB (IC_{50} 23.3 µM)	[21,76]
Chisocheton penduliflorus	Wood and leaves	Scoparone (23)	Capan-2 (IC_{50} 225.2 µM), SW1990 (IC_{50} 209.1 µM)	[22,19]
Ekebergia benguelensis	Roots barks	5-(4-hydroxyphenethenyl)-4,7-dimethoxycoumarin (26)	LNCaP (ED_{50} 22.84 µM)	[30]
		5-[(1*E*)-2-(4-hydroxyphenyl)ethenyl]-4,7-dimethoxy-3-methyl-2H-1-benzopyran-2-one (29)	Lu1 (ED_{50} 15.1 µM)	[30]
		5-[(1*E*)-2-(4-D-glucopyranosyloxyphenyl)ethenyl]-4,7-dimethoxy-3-methyl-2H-1-benzopyran-2-one (30)	Lu1 (ED_{50} >40 µM)	[30]
		1-{2-hydroxy-6-[(1*E*)-2-(4-hydroxyphenyl)ethenyl]-4-methoxyphenyl}-2- methyl-1-propanone (31)	KB (ED_{50} 31.7 µM)	[30]
		1-{2,4-dihydroxy-6-[(1*E*)-2-(4-hydroxyphenyl)ethenyl]-phenyl}-2-methyl-1-propanone (32)	LNCaP (ED_{50} 25.2 µM)	[30]
Swietenia mahagoni (L.) Jacq.	Leaves	Catechin (33)	α-Glucosidase (IC_{50} 190.2 µM), U937 (IC_{50} 11.2 µM), K562 (IC_{50} 7.1–9.1 µM), HL-60 (IC_{50} 2.34–43.5 µM)	[23,12]
Azadirachta indica var. siamensis,	Flowers	Euchrestaflavanone A (35)	A549 (IC_{50} 9.9 µM), AZ521 (IC_{50} 8.2 µM)	[32]
Azadirachta indica var. siamensis,	Flowers	4'-*O*-methyllespedezaflavanone C (36)	SK-BR-3 (IC_{50} 6.3–8.3 µM)	[32]
		3'-(3-hydroxy-3-methylbutyl)naringenin (37)	No cytotoxic activity observed	[32]
		8-prenylnaringenin (38)	HL60 (IC_{50} 35.4 µM), A549: (IC_{50} 44.4 µM), AZ521 (IC_{50} 24.7 µM), and SK-BR-3 (IC_{50} 39.4 µM)	[32]
		4'-*O*-methyl-8-prenylnaringenin (39)	HL60 (IC_{50} 4.5 µM), A549 (IC_{50} 5.4 µM), AZ521 (IC_{50} 10.5 µM), and SK-BR-3 (IC_{50} 7.9 µM)	[32]

Spesies	Part	Compound	Bioactivity result	References
		3'-prenylnaringenin (40)	HL60 (IC_{50} 20.8 μM)	[32]
Aglaia eximia	Barks	kaempferol (41)	P-388 (IC_{50} 4.26 μM)	[32]
Azadirachta indica var. siamensis,	Flowers	kaempferide (46)	HL60 (IC_{50} 43.5 μM), SK-BR-3 (IC_{50} 81.2 μM)	[32]
		3-*O*-methyl mearnsetin (47)	HL60 (IC_{50} 18.3 μM), A549 (IC_{50} 16.9 μM), AZ521 (IC_{50} 40.8 μM), and SK-BR-3 (IC_{50} 48.3 μM).	[32]
		3-methoxy-3'-prenylkaempferol (49)	HL60 (IC_{50} 6.7 μM), A549, AZ521, and SK-BR-3 (IC_{50} 16.5 – 20.0 μM)	[32]
Swietenia mahagoni (L.) Jacq.	Leaf	Quercetin-3-*O*-glucoside (56)	U937 (IC_{50} 5.45 μM), K562 (IC_{50} 5.68 μM), HL-60 (IC_{50} 6.6 μM).	[31]
Aglaia eximia	Barks	kaempferol-3-*O*-α-L-rhamnoside (67)	P-388 (IC_{50} 992.8 μM and >2312 μM)	[33]
		kaempferol-3-*O*-β-D-glucosyl-α-L-rhamnoside (68)	P-388 (IC_{50} > 1682 ± 0.17 μM)	[33]
Aglaia andamanica	Leaves	Pachypodol (73)	CaCo-2 (IC_{50} 185.6 μM) (hepatoprotective via Nrf2)	[60,61]
Melia toosendan	Fruits	Ficusal (107)	Hep3B (EC_{50} 258.5 μM)	[11,74]
		Threo-guaiacylglycerol-β-coniferyl aldehyde ether (115)	Hep3B ((2b) IC_{50} 39.02 μM, (2a) IC_{50} 67.97 μM)	[78]
		Erythro-guaiacylglycerol-β-coniferyl aldehyde ether (116)	Hep3B ((1b) IC_{50} 45.56 μM, (1a) IC_{50} 82.66 μM)	[11,78]
Aglaia elliptica	Stems	Methyl rocaglate (124)	BC1, HT-1080, and Lu1 (IC_{50} 0.0023 – 0.068 μM)	[46]
		4'-demethoxy-3',4'-methylenedioxy-methyl rocaglate (125)	ZR-75, U373 (IC_{50} 0.0018 – 0.0045 μM)	[46]
		4'-Demethoxyrocaglate (126)	BC1 (IC_{50} 0.45 μM)	[46]
		1-*O*-formyl-4'-ethylrocaglate (127)	BC1 (IC_{50} 3.18 μM)	[46]
		1-*O*-formyl-4'-demethoxy-3',4'-methylenedioxy-methyl rocaglate (128)	ZR-75 (IC_{50} 0.0023 μM)	[46]
Cedrela sinensis A. Juss	Leaves	Cedralin A (132)	HL-60 (IC_{50} 76.1 μM), K562 (IC_{50} 65.0 μM)	[47]
		Cedralin B (134)	HL-60, K562 (IC_{50} > 58 μM).	[30]

Antimicrobial

A total of 13 phenolic compounds from 5 species in 5 genera of the Meliaceae family have shown

antimicrobial potential (**Table 8**). Antimicrobial activity refers to the ability of a compound to inhibit the growth or kill microorganisms such as bacteria, fungi, and protozoa. In this study, the antimicrobial potential of several compounds isolated from *Trichilia heudelotii* was evaluated using the disc diffusion method against various microorganisms, including Gram-positive and Gram-negative bacteria, as well as some fungal strains. Among the simple phenolic compounds tested, **(5)** demonstrated stronger antibacterial activity, especially against Gram-positive bacteria, with inhibition zones of 2.43 mm (*B. subtilis*) and 2.63 mm (*M. luteus*), moderate activity against *P. aeruginosa* (2.00 mm), and mild activity against *S. aureus* (1.31 mm). No antifungal activity was observed. (1) showed a similar antimicrobial profile with slightly lower potential, with inhibition zones of 2.00 mm (*B. subtilis*), 2.03 mm (*M. luteus*), 1.53 mm (*P. aeruginosa*), and only 1.00 mm against *S. aureus*. In contrast, (6) was the most active compound in this series, with significant inhibition zones against *S. aureus* (3.31 mm) and *P. aeruginosa* (2.03 mm), moderate inhibition against *M. luteus* (2.51 mm), and *B. subtilis* (2.02 mm), demonstrating broad-spectrum antibacterial potential. Conversely, (20) showed the lowest antimicrobial activity, with limited inhibition against *B. subtilis*, *M. luteus*, and *P. aeruginosa* (each 2.00 mm), and no activity detected against *S. aureus* or other fungal strains. Overall, (6) was the most active compound, especially against *S. aureus* and *P. aeruginosa*, while (5) and (1) were more effective against Gram-positive bacteria. None of these compounds exhibited significant antifungal effects, indicating that the antimicrobial potential of these phenolic compounds is primarily antibacterial [17].

Unlike these phenolic compounds, (8), isolated from *Xylocarpus granatum*, exhibited moderate antibacterial activity against most Gram-positive bacteria and some Gram-negative bacteria, with an IC_{50} of 974.9 µM [14].

Meanwhile, (11), a new phenylpropanoid isolated from the bark of *Ekebergia senegalensis*, showed selective activity against *Staphylococcus aureus* (MIC 50 µM) and *Candida albicans* (MIC 150 µM), without causing hemolysis up to a concentration of 150 µM. Additionally, this compound demonstrated physiological effects such as smooth muscle contraction in rat bladder (EC_{50} 2.9 nM) and relaxation in rat tail arteries (EC_{50} 37.7 nM), indicating a broad spectrum of biological activity [21,62]. Furthermore, (3), also isolated from *E. senegalensis*, showed inhibitory activity against the enzyme tyrosinase with an IC_{50} of 1.23 mM. Although this potential is lower than standard inhibitors such as kojic acid (0.67 mM) and L-monimisin (0.64 mM), this compound still holds promise as a depigmentation agent for cosmetic or hyperpigmentation therapy [21].

The antimicrobial activity of the coumarin group, (19), showed moderate antiprotozoal activity against *Leishmania donovani* promastigotes (IC_{50} = 374 µM), but was inactive against *Trypanosoma brucei* and *Plasmodium falciparum*. Its cytotoxicity against KB cells was recorded with an IC_{50} of 130.2 µM, but its selectivity index (SI = 0.35) was much lower compared to pentamidine (SI = 500) [28]. Although not as strong as the positive control, this compound still demonstrates potential as an antiprotozoal and cytotoxic agent. Meanwhile, (9) from *E. senegalensis* showed limited activity, being only active against *B. subtilis* (inhibition zone 8 mm), and did not show activity against *E. coli*, *P. agarici*, *M. luteus*, or *S. warneri* [21].

In addition to antibacterial and antifungal activities, certain phenolic compounds also exhibit antiviral and antiplasmodium activities. Flavonoids such as (42) showed antiviral activity against the A/Puerto Rico/8/34 (H1N1) (IC_{50} 25.7 ± 3.6 µM), A/FM-1/47/1 (H1N1) (IC_{50} = 20.6 ± 1.6 µM), and A/Aichi/2/68 (H3N2) (IC_{50} = 9.1 ± 6.4 µM) [77]. Meanwhile, (48) and its derivatives (45) showed highly significant antiplasmodium activity with IC_{50} values ranging from 2.6 to 19.8 µM, as well as moderate cytotoxicity against HEK293T cells (IC_{50} = 64.5 ± 2.6 µM), indicating a strong potential as an antimalarial therapy candidate [34]. In contrast, (**51**) showed no activity against HIV-1 infection in C8166 cells, even at concentrations up to 250 µg/mL. These findings underscore the importance of glycosylation position on the flavonoid scaffold, where glycosylation at position C-7 tends to reduce or eliminate antiviral activity, while glycosides bound at position C-3 can retain or enhance biological activity [63].

Table 8 Antimicrobial activity of phenolic compound.

Species	Part	Compound	Bioactivity result	References
PseudoCedrela kotschyi (Schweinf.)	Roots	Quercetin (42)	H1N1 (IC_{50} 25.7 ± 3.6 and 20.6 ± 1.6 µM), H3N2 (IC_{50} = 9.1 ± 6.4 µM).	[34,77]
Ekebergia senegalensis A.	Stem barks	4-hydroxy-3,5-dimethylbenzoic acid (3)	Antibacterial: 1.0 - 2.03 mm inhibition zone	[21]
Trichilia heudelotti	Leaves	4-hydroxybenzoic acid (1)	Inhibits Gram-positive and Gram-negative bacteria (zones 1.31 - 2.63 mm)	[17]
		Protocatechuic acid (5)	*S. aureus*, *P. aeruginosa*, *M. luteus*, and *B. subtilis* (zones 2.02 - 3.31 mm); no antifungal activity	[17]
		2-methylproto-catechuic acid (6)	Antibacterial: 1.0 - 2.03 mm inhibition zone	[17]
Xylocarpus granatum	Seeds	(*E*)-4-hydroxycinnamic acid (8)	Antibacterial activity against various Gram-positive and Gram-negative bacteria (IC_{50} = 974.9 µM)	[14]
Trichilia heudelotti	Leaves	2-propionoxy-b-resorcylic acid (9)	Antibacterial activity (zone: ~2 mm); inactive against fungi	[17]
Guarea macrophylla	Leaves	Kaempferol 7-*O*-β-D-glucopyranoside (51)	HIV-1_MN in C8166 cells: Inactive up to 452.5µM Glycosylation at C-7 reduces antiviral activity	[63]
Ekebergia senegalensis A.	Stem barks	Senegalin (11)	*S. aureus* (MIC 50 µM) and *C. albicans* (MIC 150 µM) non-hemolytic, Pharmacological effect on smooth muscle and arteries	[21,62]
		4,6-dimethoxy-5-methylcoumarin (20)	*B. subtilis* (inhibition zone 8 mm), inactive against *E. coli*, *P. agarici*, *M. luteus*, *S. warneri*.	[21]
Guarea rhophalocarpa *PseudoCedrela kotschyi (Schweinf.)*	Leaves	Scopoletin (19)	*L. donovani* (IC_{50} 374 µM), inactive vs. *T. brucei* and *P. falciparum*; cytotoxic to KB cells (SI 0.35); pentamidine control (SI 500)	[28]
	Roots	3,4′,7-trimethyl esther (45)	Antiplasmodial activity (IC_{50} 64.5 ± 2.6 µM)	[34]
		3,6,8-trihydroxy-2-(3,4-dihydroxylphenyl)-4H-chrom-4-one (48)	Antiplasmodial activity (IC_{50} 2.6 – 19.8 µM)	[34]

Anti-inflammatory

Generally, only 12 compounds from 5 species in 4 genera of the Meliaceae family have demonstrated significant anti-inflammatory activity through various molecular mechanisms (**Table 9**), one of the most potent compounds, the lignan (130), exhibited strong anti-inflammatory effects without cytotoxicity at concentrations ranging from 1 to 100 µM. It significantly inhibited nitric oxide (NO) production induced by lipopolysaccharide (LPS), even more effectively than hydrocortisone, a standard anti-inflammatory drug. Moreover, (130) also suppressed the secretion of pro-inflammatory cytokines TNF-α and IL-6 in a dose-dependent manner. Its mechanism of action involves downregulating iNOS and COX-2 expression at both protein and enzymatic activity levels [64].

The simple phenolic compound (**7**), isolated from the methanolic extract of *Hyterodermia hypoleuca*, also exhibited multifaceted anti-inflammatory properties by modulating cytokine production, inhibiting key inflammatory enzymes, and suppressing signaling pathways such as NF-κB and ERK. *In vitro* studies

showed that (**7**) significantly reduced the production of NO, prostaglandin E2 (PGE2), TNF-α, and IL-6 in LPS-stimulated RAW 264.7 macrophages, and inhibited the expression of iNOS and COX-2. *In vivo*, (**7**) alleviated vasodilation and hemorrhaging in an endotoxin-induced shock model in rats, supporting its potential as a novel anti-inflammatory agent [65]. Flavonoid (70) demonstrated a comparable anti-inflammatory profile by inhibiting NO and reducing PGE2 and pro-inflammatory cytokines TNF-α, IL-6, and IL-1β in a dose-dependent manner. This effect was associated with decreased mRNA expression levels of iNOS and COX-2, indicating a transcriptional level inhibition mechanism [66].

Additionally, the neolignan (108), which accumulates in *Linum usitatissimum* cell cultures under immobilized conditions (up to 60.0 mg g^{-1} DW), exhibited pharmacological effects including anti-inflammatory and hypotensive activity, enhancing its therapeutic relevance [49]. Several other lignans also exhibited anti-inflammatory potential via NO inhibition. Compound (97) showed moderate activity (IC_{50} = 75.1 ± 2.5 μM), whereas stronger effects were observed in (98) (IC_{50} = 66.5 ± 2.2 μM), (17) (IC_{50} = 82.4 ± 1.9 μM), and 2 isomeric lignan glycosides, (92) (IC_{50} = 62.7 ± 2.3 μM) and (81) (IC_{50} = 58.0 ± 1.9 μM), all of which displayed moderate to relatively high anti-inflammatory profiles [9].

In contrast, several flavonoids from the *Aglaia* genus showed more potent NO inhibition. Compound (77) had an IC_{50} value of 24.3 ± 1.2 μM, outperforming the positive control L-NMMA (IC_{50} = 30.2 μM). Activity further increased with (78) (IC_{50} = 22.7 ± 1.4 μM) and peaked with (79) (IC_{50} = 21.4 ± 1.2 μM), which was the most effective compound in suppressing NO production [9]. Overall, lignans such as (130) and flavonoids like (79) stand out as the most potent anti-inflammatory agents identified in this study. These findings highlight the importance of chemical structure in modulating anti-inflammatory activity, with furofuran-type lignans and selected flavonoids demonstrating the highest potential.

Table 9 Antiinflamation activity of phenolic compound.

Species	Part	Compound	Bioactivity result	References
Ekebergia capensis	Barks	Atraric acid (7)	Inhibits NO, PGE2, TNF-α, IL-6; downregulates iNOS, COX-2, NF-κB, and ERK	[65]
Aglaia odorata Lour.	Leaves	(+)-Ent-ficusol (17)	NO: IC_{50} 82.4 ± 1.9 μM	[9]
Aglaia andamanica	Leaves	5-hydroxy-3,4',7,-trimethoxyflavone (71)	Inhibits NO, PGE2, TNF-α, IL-6, IL-1β; downregulates iNOS & COX-2 mRNA	[66]
Aglaia odorata Lour.	Leaves	Aglaodoratas A (77)	NO inhibition (IC_{50} 24.3 ± 1.2 μM), L-NMMA (IC_{50} 30.2 μM)	[9]
		Aglaodoratas B (78)	NO inhibition (IC_{50} 22.7 ± 1.4 μM)	[9]
		Aglaodoratas C (79)	NO inhibition (IC_{50} 21.4 ± 1.2 μM)	[9]
		(−)-isolarisiresinol 3α-*O*-β-D-glucopyranoside (81)	NO inhibition (IC_{50} 58.0 ± 1.9 μM)	[9]
		(+)-isolarisiresinol 3α-*O*-β-D-glucopyranoside (92)	NO inhibition (IC_{50} 62.7 ± 2.3 μM; moderate activity	[9]
		Forsythoside A (97)	NO inhibition (IC_{50} 75.1 ± 2.5 μM)	[9]
		Caruilignan C (98)	NO inhibition (IC_{50} 66.5 ± 2.2 μM)	[9]
Guarea macrophylla	Leaves	Dehydrodiconiferyl alcohol-4-β-D-glucoside (109)	Anti-inflammatory, hypotensive; accumulates in *L. usitatissimum* (60 mg/g DW)	[67]

Species	Part	Compound	Bioactivity result	References
Melia toosendan	Fruits	Picrasmalignan A (130)	Inhibits NO, TNF-α, IL-6; downregulates iNOS & COX-2; non-cytotoxic (1 - 100 μM); more effective than hydrocortisone.	[64]

Serotonin receptor agonistic activity

Agonistic activity refers to the ability of a compound to bind and activate specific receptors, mimicking the action of endogenous ligands (**Table 10**). In this study, 8 lignans (99, 119 - 122, 130, 132, 105) isolated from *Melia toosendan* were evaluated for their agonistic activity at serotonin receptors 5-HT1A and 5-HT2C. (119) shows weak activity at both receptors, with 4.28% at 5-HT1A and 6.94% at 5-HT2C. (122) demonstrates higher agonistic activity, especially at 5-HT1A (21.16%) and moderate activity at 5-HT2C (9.80%). (120) activates only 5-HT1A (5.08%) and shows no detectable activity at 5-HT2C. In contrast, (121) shows selective activity at 5-HT2C (11.39%) with no activity at 5-HT1A. (129) exhibits moderate dual activity at both receptors (8.04 and 10.28%, respectively). (131) shows very limited activity, only at 5-HT2C (7.73%). (99) demonstrates relatively high activity at 5-HT1A (37.55%) and none at 5-HT2C, indicating selectivity towards this receptor. Among all compounds, (105) shows the strongest agonistic activity at 5-HT1A (57.77%) and notable activity at 5-HT2C (14.88%). These findings suggest that lignans from *M. toosendan* have potential as modulators of the serotonin system, particularly as agonists of the 5-HT1A receptor [11].

Table 10 Serotonin receptor agonistic activity of phenolic compound.

Species	Part	Compound	Bioactivity result	References
Melia toosendan	Fruits	(2*R*,3*R*,4*S*)-2,3-Diguaiacyl-4-hydroxyl tetrahydrofuran (99)	5-HT1A (37.55%), undetectable on 5-HT2C	[11]
		(+)-pinoresinol (105)	5-HT1A (57.77%), 5-HT2C (14.88%)	[11]
		Threo-Guaiacylethoxyglycerol-β-*O*-4′-coniferyl aldehyde ether (119)	5-HT1A (4.28%), 5-HT2C (6.94%)	[11]
		Threo-Guaiacylethoxyglycerol-β-*O*-4′-guaiacyl aldehyde ether (120)	5-HT1A (5.08%), undetectable on 5-HT2C	[11]
		Erythro-Guaiacylethoxyglycerol-β-*O*-4′-guaiacyl aldehyde ether (121)	5-HT2C (11.39%), inactive on 5-HT1A	[11]
		Erythro-Guaiacylethoxyglycerol-β-*O*-4′-coniferyl aldehyde ether (122)	5-HT1A (21.16%), 5-HT2C (9.80%)	[11]
		Trans-2-Guaiacyl-3-hydroxymethyl-5-(cis-3′-hydroxymethyl-5′-formyl-7′-methoxybenzofuranyl)-7-methoxybenzofuran (129)	5-HT1A (8.04%), 5-HT2C (10.28%)	[11]
		Erythro-Guaiacylglycerol-β-*O*-4′-(+)-5,5′-dimethoxylariciresinol ether (131)	5-HT2C (7.73%)	[11]

Conclusions

Recent investigations up to 2024 have highlighted the chemical diversity and therapeutic promise of phenolic compounds from the Meliaceae family. These include lignans, flavonoids, simple phenolics, coumarins, and stilbenoids, with lignans being the most prevalent group (46.3%). Phenolics from this family display broad biological activities antioxidant,

cytotoxic, anti-inflammatory, antimicrobial, and serotonin receptor agonistic supporting their potential as natural drug leads.

To exemplify this potential, several compounds stand out. Cinchonain Ic (142) and Id (143) showed excellent antioxidant capacity with IC_{50} values of 2.5 and 2.3 μM, respectively. Rocaglate-type lignans such as Methyl rocaglate (124) and its derivative (125) demonstrated potent cytotoxicity in the nanomolar range (IC_{50} = 0.0023 – 0.068 μM). 2-methylproto-catechuic acid (6) exhibited the highest antibacterial activity with a 3.31 mm inhibition zone against *S. aureus*. In terms of anti-inflammatory action, Picrasmalignan A (130) inhibited NO and proinflammatory cytokines more effectively than hydrocortisone without cytotoxicity, and Aglaodoratas C (79) showed the strongest NO inhibition among flavonoids (IC_{50} = 21.4 μM). As serotonin receptor agonists, (+)-Pinoresinol (105) showed high activity at 5-HT1A (57.77%) and moderate at 5-HT2C (14.88%), while (2R,3R,4S)-2,3-diguaiacyl-4-hydroxyl tetrahydrofuran (99) selectively activated 5-HT1A (37.55%). While Meliaceae phenolics exhibit strong therapeutic promise, numerous phenolic compounds from other plant families such as Fabaceae, Asteraceae, and Lauraceae have also been reported with potent bioactivities. However, their diversity and mechanisms remain underexplored in comparison. Future studies should deepen investigation into their biochemical pathways, biosynthetic origins, and structure-activity relationships (SAR), and expand phytochemical screening across broader taxa to unlock new drug discovery opportunities.

Acknowledgements

The authors are grateful to the Universitas Padjadjaran, Indonesia, for the Assignment Research Grant, No: 1146/UN6.3.1/PT.00/2025 provided by Unang Supratman.

Declaration of Generative AI in Scientific Writing

The authors recognize that generative AI tools (such as ChatGPT by OpenAI) were employed during the preparation of this manuscript exclusively for improving language clarity and grammar. The AI was not used for generating content or interpreting data. The authors retain full responsibility for the manuscript's content and conclusions.

CRediT Author Statement

Hikma Ainazzahra: Conceptualization, Methodology, Data extraction, Data curation, Visualization, Writing – original draft.

Citra Nisa Ul Inayah: Data extraction, Data curation, Visualization, Writing – original draft.

Al Arofatus Naini: Methodology, Supervision, Validation, Resources.

Kindi Farabi: Supervision, Validation, Draft editing.

Desi Harneti: Supervision, Validation, Draft editing.

Unang Supratman: Supervision, Project administration, Funding acquisition, Resources.

References

[1] AN Muellner-Riehl and BM Rojas-Andrés. Biogeography of neotropical Meliaceae: Geological connections, fossil and molecular evidence revisited. *Brazilian Journal of Botany* 2022; **45(1)**, 527-543.

[2] TT Hieu, PT Thuy and DX Duc. Isolation and bioactivities of limonoids from *Meliaceae* family: A review. *Current Organic Chemistry* 2022; **26(14)**, 1359-1430.

[3] U Supratman, W Naibaho, S Salam, R Maharani, AT Hidayat, D Harneti, Nurlelasari and Y Shiono. Cytotoxic triterpenoids from the bark of *Chisocheton patens* Blume (Meliaceae). *Phytochemistry Letters* 2019; **30**, 81-87.

[4] SA Riyadi, AA Naini and U Supratman. Sesquiterpenoids from Meliaceae family and their biological activities. *Molecules* 2023; **28(12)**, 4874.

[5] Supriatno, Nurlelasari, T Herlina, D Harneti, R Maharani, AT Hidayat, T Mayanti, U Supratman, MN Azmi and Y Shiono. A new limonoid from stem bark of *Chisocheton pentandrus* (Meliaceae). *Natural Product Research* 2018; **32(21)**, 2610-2616.

[6] SA Riyadi, AA Naini, T Mayanti, R Lesmana, MN Azmi, S Fajriah, S Jungsuttiwong and U Supratman. Alliaxylines A-E: Five new mexicanolides from the stem barks of *Dysoxylum alliaceum* (Blume) Blume ex A. Juss. *Journal of Natural Medicines* 2024; **78(3)**, 558-567.

[7] AA Naini, T Mayanti, R Maharani, D Harneti, Nulelasari, K Farabi, S Fajriah, Hilmayanti, K

Kabayama, A Shimoyama, Y Manabe, K Fukase, S Jungsuttiwong, TAK Prescott and U Supratman. Paraxylines AG: Highly oxygenated preurianin-type limonoids with immunomodulatory TLR4 and cytotoxic activities from the stem bark of *Dysoxylum parasiticum*. *Phytochemistry* 2024; **220**, 114009.

[8] R Ahmad, N Ahmad, AA Naqvi, V Exarchou, A Upadhyay, E Tuenter, K Foubert, S Apers, N Hermans and L Pieters. Antioxidant and antiglycating constituents from leaves of *Ziziphus oxyphylla* and *Cedrela serrata*. *Antioxidants* 2016; **5(1)**, 9.

[9] PH Yen, NA Bang, DTH Yen, DT Dung, PTT Huong, NH Hoang, BH Tai, LT Anh and PV Kiem. Undescribed 2,9-deoxyflavonoids and flavonol-diamide [3+2] adduct from the leaves of *Aglaia odorata* Lour. inhibit nitric oxide production. *Phytochemistry* 2023; **214**, 113792.

[10] NKT Dharmayani, T Yoshimura, E Hermawati, LD Juliawaty and YM Syah. Antibacterial and antifungal two phenolic sesquiterpenes from *Dysoxylum densiflorum*. *Zeitschrift für Naturforschung C* 2020; **75(1-2)**, 1-5.

[11] H Wang, CA Geng, HB Xu, XY Huang, YB Ma, CY Yang, XM Zhang and JJ Chen. Lignans from the fruits of *Melia toosendan* and their agonistic activities on melatonin receptor MT1. *Planta Medica* 2015; **81(10)**, 847-854.

[12] B Elya, FS Budiarso, M Hanafi, MA Gani and PW Prasetyaningrum. Two tetrahydroxyterpenoids and a flavonoid from *Xylocarpus moluccensis* M.Roem. and their α-glucosidase inhibitory and antioxidant capacity. *Journal of Pharmacy and Pharmacognosy Research* 2024; **12(3)**, 453-476.

[13] L Peng, WX Fu, CX Zeng, L Zhou, MF Bao and XH Cai. Two new lignans from twigs of *Aglaia odorata*. *Journal of Asian Natural Products Research* 2016; **18(2)**, 147-152.

[14] JY Cho, JH Moon, KY Seong and KH Park. Antimicrobial activity of 4-hydroxybenzoic acid and trans 4-hydroxycinnamic acid isolated and identified from rice hull. *Bioscience, Biotechnology, and Biochemistry* 1998; **62(11)**, 2273-2276.

[15] L Wang, F Li, CY Yang, AA Khan, X Liu and MK Wang. Neolignans, lignans and glycoside from the fruits of *Melia toosendan*. *Fitoterapia* 2014; **99**, 92-98.

[16] ME Cartea, M Francisco, P Soengas and P Velasco. Phenolic compounds in *Brassica* vegetables. *Molecules* 2010; **16(1)**, 251-280.

[17] AJ Aladesanmi and SA Odediran. Antimicrobial activity of *Trichilia heudelotti* leaves. *Fitoterapia* 2000; **71(2)**, 179-182.

[18] Q Li, F Song, M Zhu, Q Wang, Y Han, Y Ling, L Qiao, N Zhong and L Zhang. Hyperoside: A review of pharmacological effects. *F1000 Research* 2022; **11**, 635.

[19] O Myint, S Wattanapongpitak, S Kothan, C Udomtanakunchai, S Tima and M Tungjai. Modulation of p-glycoprotein-mediated efflux pirarubicin in living multidrug-resistant K562/Dox cell lines by 4-hydroxybenzoic acid and 4-hydroxy-3-methoxybenzoic acid via impairment of the cellular energetic state. *Toxicology Reports* 2022; **9**, 1443-1451.

[20] MS Abdelfattah, K Toume, F Ahmed, SK Sadhu and M Ishibashi. Cucullamide, a new putrescine bisamide from *Amoora cucullata*. *Chemical and Pharmaceutical Bulletin* 2010; **58(8)**, 1116-1118.

[21] GPM Kemayou, GM Happi, YAT Ngandjui, JC Tchouankeu, N Sewald, MS Ali and SF Kouam. Senegalin, a new phenylpropanoid and other secondary metabolites from the stem bark of *Ekebergia senegalensis A. Juss*. (Meliaceae). *Natural Product Research* 2021; **35(21)**, 3694-3700.

[22] J Phongmaykin, T Kumamoto, T Ishikawa, R Suttisri and E Saifah. A new sesquiterpene and other terpenoid constituents of *Chisocheton penduliflorus*. *Archives of Pharmacal Research* 2008; **31**, 21-27.

[23] DA Mulholland, HA Mahomed and S Iourine. A comparison of extractives from the bark of *Ekebergia capensis* and *Ekebergia senegalensis*. *South African Journal of Botany* 1997; **63(5)**, 259-260.

[24] MY Li, XB Yang, JY Pan, G Feng, Q Xiao, J Sinkkonen, T Satyanandamurty and J Wu. Granatumins A-G, limonoids from the seeds of a krishna mangrove, *Xylocarpus granatum*. *Journal of Natural Products* 2009; **72(12)**, 2110-2114.

[25] KJ Wang, CR Yang and YJ Zhang. Phenolic antioxidants from Chinese toon (fresh young leaves and shoots of *Toona sinensis*). *Food Chemistry* 2007; **101(1)**, 365-371.

[26] SK Sadhu, P Phattanawasin, MSK Choudhuri, T Ohtsuki and M Ishibashi. A new lignan from *Aphanamixis polystachya*. *Journal of Natural Medicines* 2006; **60(3)**, 258-260.

[27] JY Salib, HN Michael and SI El-Nogoumy. New lactoyl glycoside Quercetin from *Melia azedarach* leaves. *Chemistry of Natural Compounds* 2008; **44**, 13-15.

[28] MDR Camacho, JD Phillipson, SL Croft, GC Kirby, DC Warhurst and PN Solis. Terpenoids from *Guarea rhophalocarpa*. *Phytochemistry* 2001; **56(2)**, 203-210.

[29] BS Siddiqui, M Rasheed, F Ilyas, T Gulzar, RM Tariq and SNUH Naqvi. Analysis of insecticidal *Azadirachta indica* A. Juss. fractions. *Zeitschrift für Naturforschung C* 2004; **59(1-2)**, 104-112.

[30] D Chávez, HB Chai, TE Chagwedera, Q Gao, NR Farnsworth, GA Cordell, JM Pezzuto and AD Kinghorn. Novel stilbenes isolated from the root bark of *Ekebergia benguelensis*. *Tetrahedron Letters* 2001; **42(22)**, 3685-3688.

[31] S Roy, B Banerjee and JR Vedasiromoni. Cytotoxic and apoptogenic effect of *Swietenia mahagoni* (L.) Jacq. leaf extract in human leukemic cell lines U937, K562 and HL-60. *Environmental Toxicology and Pharmacology* 2014; **37(1)**, 234-247.

[32] W Kitdamrongtham, K Ishii, K Ebina, J Zhang, M Ukiya, K Koike, H Akazawa, A Manosroi and T Akihisa. Limonoids and flavonoids from the flowers of *Azadirachta indica* var. siamensis, and their melanogenesis-inhibitory and cytotoxic activities. *Chemistry and Biodiversity* 2014; **11(1)**, 73-84.

[33] J Sianturi, M Purnamasari, T Mayanti, D Harneti, U Supratman, K Awang and H Hayashi. Flavonoid compounds from the bark of *Aglaia eximia* (Meliaceae). *Makara Journal of Science* 2015; **19(1)**, 2.

[34] LS Sidjui, YOD Nganso, RMK Toghueo, BNK Wakeu, JT Dameue, P Mkounga, A Adhikari, M Lateef, GN Folefoc and MS Ali. Kostchyienones A and B, new antiplasmodial and cytotoxicity of limonoids from the roots of*Pseudocedrela kotschyi* (Schweinf.) Harms. *Zeitschrift für Naturforschung C* 2018; **73(3-4)**, 153-160.

[35] SA Jain and SK Srivastava. 8-c-methyl-quercetin-3-o-β/-d-xylopyranoside, a new flavone glycoside from the roots of *Amoora rohituka*. *Journal of Natural Products* 1985; **48(2)**, 299-301.

[36] J Puripattanavong, S Weber, V Brecht and AW Frahm. Phytochemical investigation of *Aglaia andamanica*. *Planta Medica* 2000; **66(8)**, 740-745.

[37] C Pereira, CBB Júnior, RM Kuster, NK Simas, CM Sakuragui, A Porzel and L Wessjohann. Flavonoids and a neolignan glucoside from *Guarea macrophylla* (Meliaceae). *Química Nova* 2012; **35**, 1123-1126.

[38] W Tang, H Hioki, K Harada, M Kubo and Y Fukuyama. Antioxidant phenylpropanoid-substituted epicatechins from *Trichilia catigua*. *Journal of Natural Products* 2007; **70(12)**, 2010-2013.

[39] K He, BN Timmermann, AJ Aladesanmi and L Zeng. A biflavonoid from *Dysoxylum lenticellare* gillespie. *Phytochemistry* 1996; **42(4)**, 1199-1201.

[40] RB Teponno, S Kusari and M Spiteller. Recent advances in research on lignans and neolignans. *Natural Product Reports* 2016; **33(9)**, 1044-1092.

[41] SP Voravuthikunchai, T Kanchanapoom, N Sawangjaroen and N Hutadilok-Towatana. Antioxidant, antibacterial and antigiardial activities of *Walsura robusta* Roxb. *Natural Product Research* 2010; **24(9)**, 813-824.

[42] DAG Cortez, JB Fernandes, QB Cass, PC Vieira, MFGD Silva, AG Ferreira and JR Pirani. Lignan glycosides from *Trichilia estipulata* bark. *Natural Product Letters* 1998; **11(4)**, 255-262.

[43] J Sianturi, D Harneti, Darwati, T Mayanti, U Supratman and K Awang. A New (-)-5′,6-dimethoxyisolariciresinol-(3″,4″-dimethoxy)-3α-O-β-d-glucopyranoside from the bark of *Aglaia eximia* (Meliaceae). *Natural Product Research* 2016; **30(19)**, 2204-2208.

[44] BG Wang, H Peng, HL Huang, XM Li, G Eck, X Gong and P Proksch. Rocaglamide, aglain, and other related derivatives from *Aglaia testicularis* (Meliaceae). *Biochemical Systematics and Ecology* 2004; **32(12)**, 1223-1226.

[45] N Fuzzati, W Dyatmiko, A Rahman, F Achmad and K Hostettmann. Triterpenoids, lignans and a benzofuran derivative from the bark of *Aglaia elaeagnoidea*. *Phytochemistry* 1996; **42(5)**, 1395-1398.

[46] SK Lee, B Cui, RR Mehta, AD Kinghorn and JM Pezzuto. Cytostatic mechanism and antitumor potential of novel 1H-cyclopenta[b]benzofuran lignans isolated from *Aglaia elliptica*. *Chemico-Biological Interactions* 1998; **115(3)**, 215-228.

[47] IS Lee, HJ Kim, UJ Youn, QC Chen, JP Kim, DT Ha, TM Ngoc, BS Min, SM Lee, HJ Jung, MK Na and KH Bae. Dihydrobenzofuran norlignans from the leaves of *Cedrela sinensis* A. Juss. *Helvetica Chimica Acta* 2010; **93(2)**, 272-276.

[48] DR Kar, P Ghosh, P Suresh, S Chandra and D Paul. Review on phyto-chemistry & pharmacological activity of *Melia azedarach*. *International Journal of Experimental Research and Review* 2022; **28**, 38-46.

[49] TJ Hsieh, TZ Liu, YC Chia, CL Chern, FL Lu, MC Chuang, SY Mau, SH Chen, YH Syu and CH Chen. Protective effect of methyl gallate from *Toona sinensis* (Meliaceae) against hydrogen peroxide-induced oxidative stress and DNA damage in MDCK cells. *Food and Chemical Toxicology* 2004; **42(5)**, 843-850.

[50] CAVD Heijden, PJ Janssen and JJ Strik. Toxicology of gallates: A review and evaluation. *Food and Chemical Toxicology* 1986; **24(10-11)**, 1067-1070.

[51] SA Pshenichnyuk, YN Elkin, NI Kulesh, EF Lazneva and AS Komolov. Low-energy electron interaction with retusin extracted from *Maackia amurensis*: Towards a molecular mechanism of the biological activity of flavonoids. *Physical Chemistry Chemical Physics* 2015; **17(26)**, 16805-16812.

[52] WJ Choung, SH Hwang, DS Ko, SB Kim, SH Kim, SH Jeon, HD Choi, SS Lim and JH Shim. Enzymatic synthesis of a novel kaempferol-3-O-β-D-glucopyranosyl-(1→4)-O-α-D-glucopyranoside using cyclodextrin glucanotransferase and its inhibitory effects on aldose reductase, inflammation, and oxidative stress. *Journal of Agricultural and Food Chemistry* 2017; **65(13)**, 2760-2767.

[53] A Szakiel, L Voutquenne-Nazabadioko and M Henry. Isolation and biological activities of lyoniside from rhizomes and stems of *Vaccinium myrtillus*. *Phytochemistry Letters* 2011; **4(2)**, 138-143.

[54] X Li, W Cao, Y Shen, N Li, XP Dong, KJ Wang and YX Cheng. Antioxidant compounds from *Rosa laevigata* fruits. *Food Chemistry* 2012; **130(3)**, 575-580.

[55] CW Song, SM Wang, LL Zhou, FF Hou, KJ Wang and QB Han. Isolation and identification of compounds responsible for antioxidant capacity of Euryale ferox seeds. *Journal of Agricultural and Food Chemistry* 2011; **59(4)**, 1199-1204.

[56] Y Yu, ZB Wang, YD Zhai, PY Song, QH Wang, BY Yang and HX Kuang. Lignan glycosides from *Gentianella acuta* (Michx.) Hultén. and their protective effects against H_2O_2-induced apoptosis in H9c2 cardiomyoblasts. *Records of Natural Products* 2014; **8(3)**, 234-241.

[57] J Xiong, VB Bui, XH Liu, ZL Hong, GX Yang and JF Hu. Lignans from the stems of *Clematis armandii* ("Chuan-Mu-Tong") and their anti-neuroinflammatory activities. *Journal of Ethnopharmacology* 2014; **153(3)**, 737-743.

[58] JJ Chen, HB Wei, YZ Xu, J Zeng and K Gao. Antioxidant lignans from the roots of *Vladimiria muliensis*. *Planta Medica* 2013; **79(15)**, 1470-1473.

[59] K Prasad. Antioxidant activity of secoisolariciresinol diglucoside-derived metabolites, secoisolariciresinol, enterodiol, and enterolactone. *International Journal of Angiology* 2000; **9(4)**, 220-225.

[60] HA Ali, AKA Chowdhury, AKM Rahman, T Borkowski, L Nahar and SD Sarker. Pachypodol, a flavonol from the leaves of *Calycopteris floribunda*, inhibits the growth of CaCo2 colon cancer cell line *in vitro*. *Phytotherapy Research* 2008; **22(12)**, 1684-1687.

[61] EK Kim, JH Kim, S Jeong, YW Choi, HJ Choi, CY Kim and YM Kim. Pachypodol, a methoxyflavonoid isolated from *Pogostemon cablin* Bentham exerts antioxidant and cytoprotective effects in HepG2 cells: Possible role of ERK-dependent Nrf2 activation.

International Journal of Molecular Sciences 2019; **20(17)**, 4082.

[62] H Wang, R Li, X Xi, T Meng, M Zhou, L Wang, Y Zhang, T Chen and C Shaw. Senegalin: A novel antimicrobial/myotropic hexadecapeptide from the skin secretion of the African running frog, *Kassina senegalensis*. *Amino Acids* 2013; **44(5)**, 1347-1355.

[63] N Mahmood, S Piacente, C Pizza, A Burke, AI Khan and AJ Hay. The anti-HIV activity and mechanisms of action of pure compounds isolated from *Rosa damascena*. *Biochemical and Biophysical Research Communications* 1996; **229(1)**, 73-79.

[64] F Zhao, L Chen, C Bi, M Zhang, W Jiao and X Yao. *In vitro* anti-inflammatory effect of picrasmalignan A by the inhibition of iNOS and COX-2 expression in LPS-activated macrophage RAW 264.7 cells. *Molecular Medicine Reports* 2013; **8(5)**, 1575-1579.

[65] SK Mun, KY Kang, HY Jang, YH Hwang, SG Hong, SJ Kim, HW Cho, DJ Chang, JS Hur and ST Yee. Atraric acid exhibits anti-inflammatory effect in lipopolysaccharide-stimulated RAW264.7 cells and mouse models. *International Journal of Molecular Sciences* 2020; **21(19)**, 7070.

[66] A Sudha, J Jeyakanthan and P Srinivasan. Protective effect of 5-hydroxy-3′,4′,7-trimethoxyflavone against inflammation induced by lipopolysaccharide in RAW 264.7 macrophage: *In vitro* study and *in silico* validation. *Medical Chemistry Research* 2016; **25**, 1754-1767.

[67] J Attoumbré, S Charlet, S Baltora-Rosset, C Hano, SRL Grandic, F Gillet, L Bensaddek, F Mesnard and MA Fliniaux. High accumulation of dehydrodiconiferyl alcohol-4-β-D-glucoside in free and immobilized *Linum usitatissimum* cell cultures. *Plant Cell Reports* 2006; **25**, 859-864.

[68] L Hu, XM Tian, CC Wang, Q Olga, D Yan, PF Tang, LN Zhang, LY Kong and J Luo. New triterpenoids, steroids and lignan from the stem barks of *Entandrophragma utile*. *Fitoterapia* 2020; **143**, 104546.

[69] SM Yang, QS Song, C Qing, DG Wu and XK Liu. Anticancer activity of tirucallane triterpenoids from *Amoora dasyclada*. *Zeitschrift für Naturforschung C* 2006; **61(3-4)**, 193-195.

[70] WDS Terra, IJC Vieira, R Braz-Filho, WRD Freitas, MM Kanashiro and MCM Torres. Lepidotrichilins A and B, new protolimonoids with cytotoxic activity from *Trichilia lepidota* (Meliaceae). *Molecules* 2013; **18(10)**, 12180-12191.

[71] SA Jonker, MHH Nkunya, L Mwamtobe, J Geenevasen and GJ Koomen. A new coumarin and polyhydroxysqualenes from *Ekebergia benguelensis*. *Natural Product Letters* 1997; **10(4)**, 245-248.

[72] BN Irungu, JA Orwa, A Gruhonjic, PA Fitzpatrick, G Landberg, F Kimani, J Madiwo, M Erdélyi and A Yenesew. Constituents of the roots and leaves of *Ekebergia capensis* and their potential antiplasmodial and cytotoxic activities. *Molecules* 2014; **19(9)**, 14235-14246.

[73] T Murata, T Miyase, FW Muregi, Y Naoshima-Ishibashi, K Umehara, T Warashina and A Ishih. Antiplasmodial triterpenoids from *Ekebergia capensis*. *Journal of Natural Products* 2008; **71(2)**, 167-174.

[74] FP Chang, W Chao, SY Wang, HC Huang, PJ Sung, JJ Chen, MJ Cheng, GJ Huang and YH Kuo. Three new iridoid derivatives have been isolated from the stems of *Neonauclea reticulata* (Havil.) Merr. with cytotoxic activity on hepatocellular carcinoma cells. *Molecules* 2018; **23(9)**, 2297.

[75] N Li, F Yang, DY Liu, JT Guo, N Ge and SY Sun. Scoparone inhibits pancreatic cancer through PI3K/Akt signaling pathway. *World Journal of Gastrointestinal Oncology* 2021; **13(9)**, 1164-1183.

[76] H Morita, T Dota and J Kobayashi. Antimitotic activity of glaupalol-related coumarins from *Glaucidium palmatum*. *Bioorganic and Medical Chemistry Letters* 2004; **14(14)**, 3665-3668.

[77] W Wu, R Li, X Li, J He, S Jiang, S Liu and L Yang. Quercetin as an antiviral agent inhibits Influenza A virus (IAV) entry. *Viruses* 2015; **8(1)**, 6.

[78] GD Yao, J Wang, XY Song, L Zhou, LL Lou, WY Zhao, B lin, XX Huang and SJ Song. Stereoisomeric guaiacylglycerol-β-coniferyl aldehyde ether induces distinctive apoptosis by

downregulation of MEK/ERK pathway in hepatocellular carcinoma cells. *Bioorganic Chemistry* 2018; **81**, 382-388.

Structures

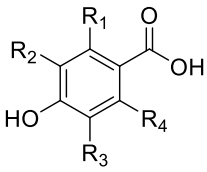

1 R_1=H, R_2=H, R_3=H, R_4=H
2 R_1=H, R_2=OMe, R_3=H, R_4=H
3 R_1=H, R_2=Me, R_3=Me, R_4=H
4 R_1=H, R_2=OH, R_3=OH, R_4=H
5 R_1=H, R_2=H, R_3=OH, R_4=H
6 R_1=Me, R_2=OH, R_3=H, R_4=H

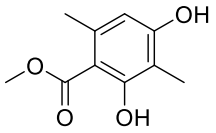

7

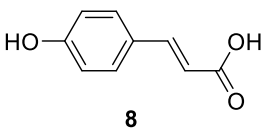

8

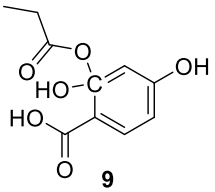

9

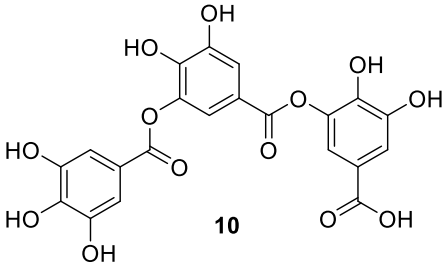

10

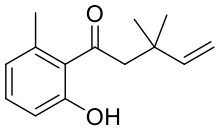

11

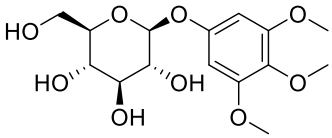

12

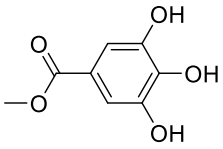

14

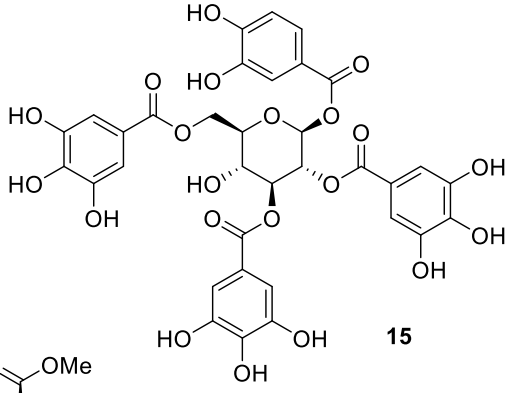

15

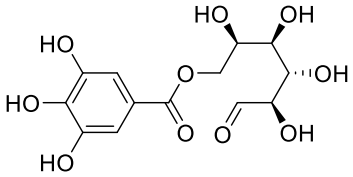

13

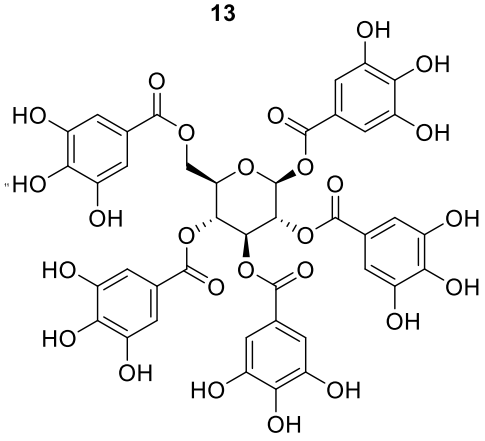

16

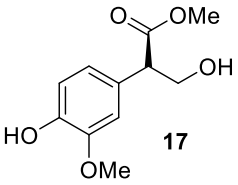

17

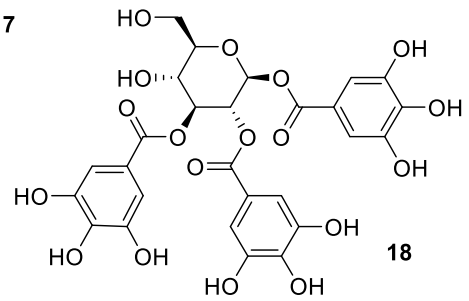

18

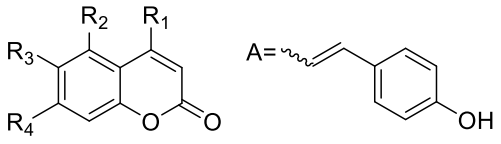

19 R_1=R_2=H, R_3=OMe, R_4=OH
20 R_1=OMe, R_2=Me, R_3=OMe, R_4=H
21 R_1=OMe, R_2=Me, R_3=OH, R_4=H
22 R_1=OMe, R_2=CH_2OH, R_3=R_4=H
23 R_1=R_2=H, R_3=OMe, R_4=OMe
24 R_1=OMe, R_2=Me, R_3=R_4=H
25 R_1=R_2=Me, R_3=R_4=H
26 R_1=OMe, R_2=A, R_3=H, R_4=OMe

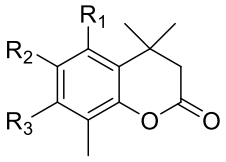

27 R_1=Me, R_2=R_3=H
28 R_1=H, R_2=OH, R_3=Me

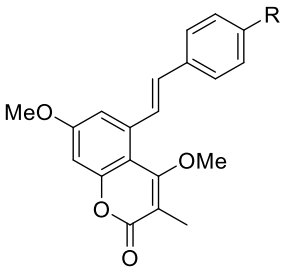

29 R = OH
30 R = OGlc

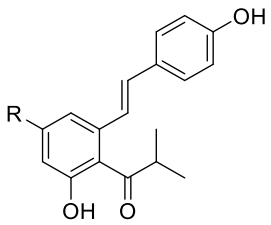

31 R = OMe
32 R = OH

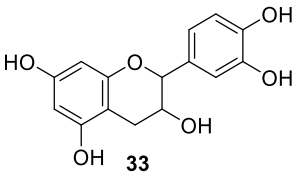

33

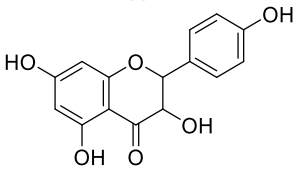

34

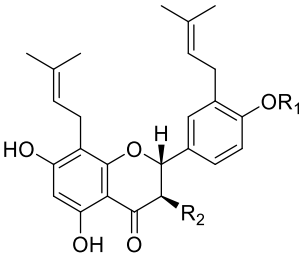

35 R_1=R_2=H
36 R_1=OH, R_2=Me

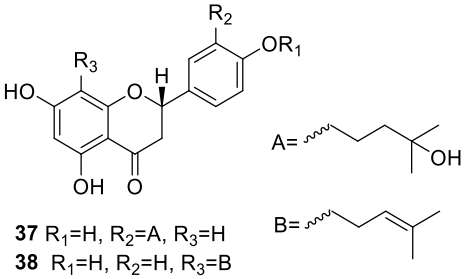

37 R_1=H, R_2=A, R_3=H
38 R_1=H, R_2=H, R_3=B
39 R_1=Me, R_2=H, R_3=B
40 R_1=H, R_2=B, R_3=H

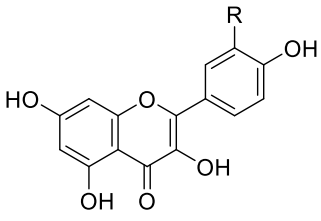

41 R=H
42 R=OH

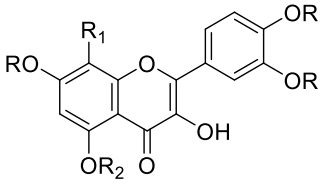

43 R=R_2=H, R_1=Me
44 R=R_2=Me, R_1=Me
45 R=Me, R_1=R_2=H

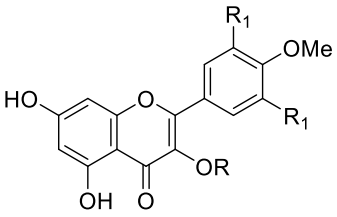

46 R=R_1=H
47 R=Me R_1=OH

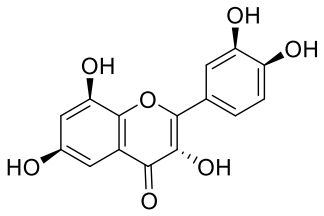

48

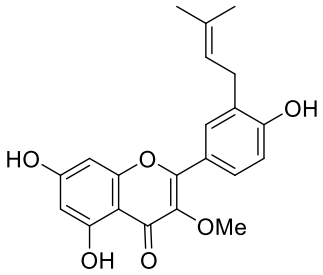

49

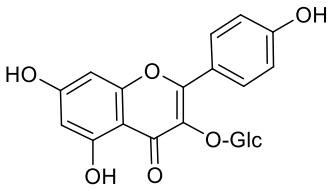

50

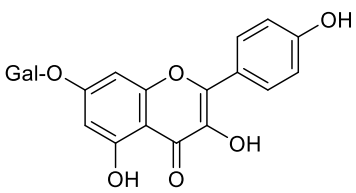

51

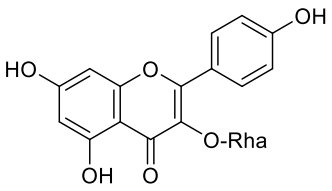

52

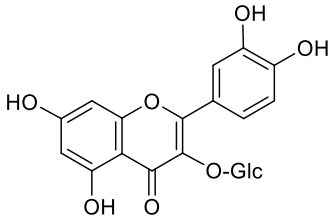

53

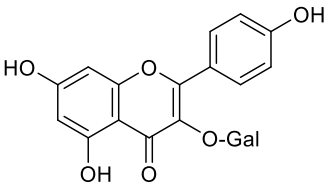

54

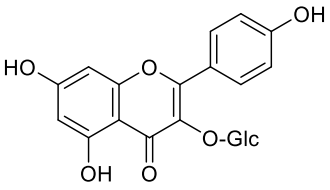

55

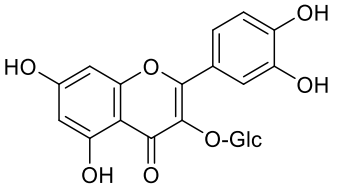

56

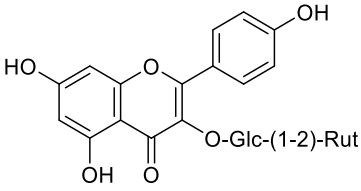

57

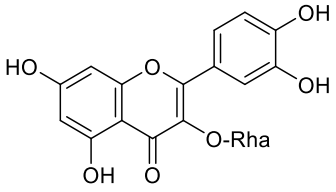

58

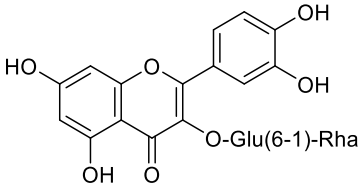

59

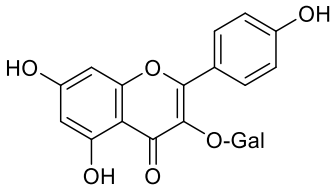

60

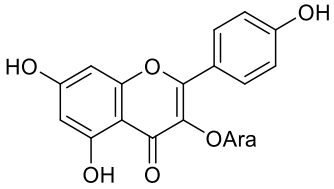

61

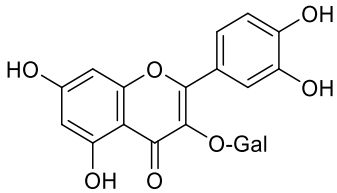

62

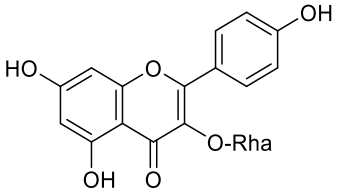

63

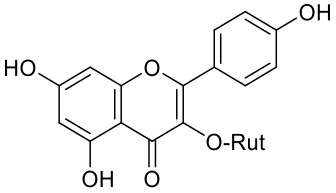

64

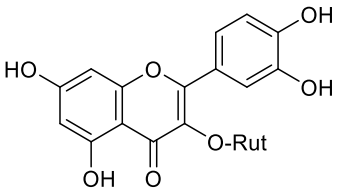

65

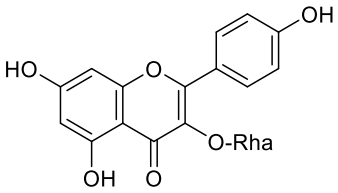

66

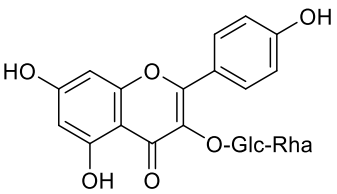

67

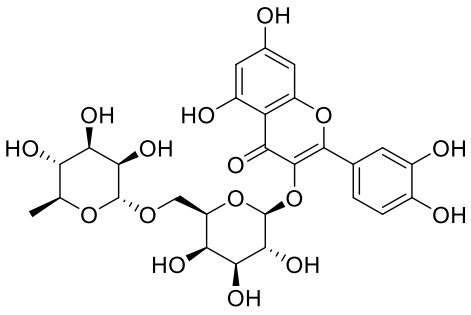

68

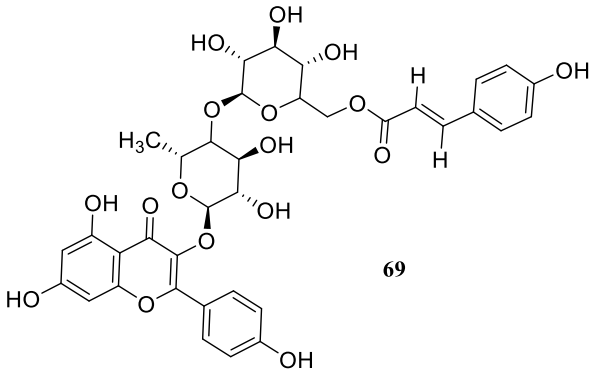

69

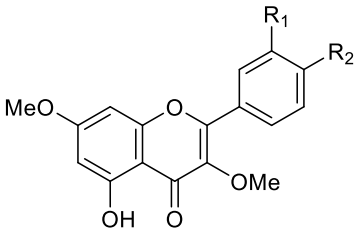

70 R_1=H, R_2=OMe
71 R_1=OMe, R_2=OMe
72 R_1=OMe: R_2=OH

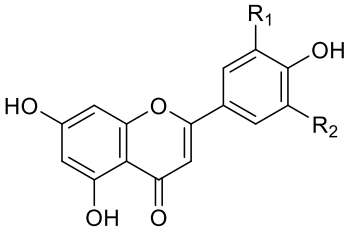

73 R_1= H R_2= H
74 R_1= OMe R_2= OMe

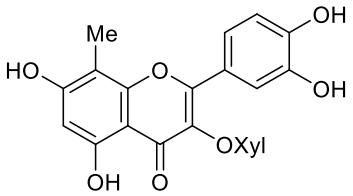

75

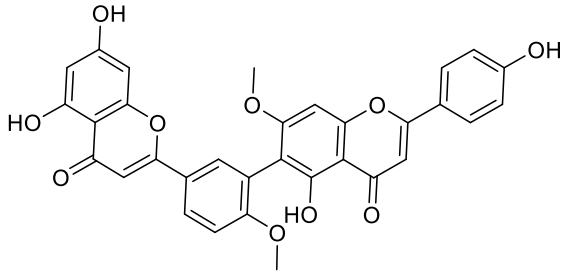

76

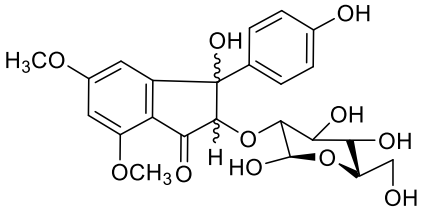

77 β-OH, β-H:(2R,3S)
78 β-OH, α-H:(2R,3R)
79 α-OH, α-H:(2S,3R)

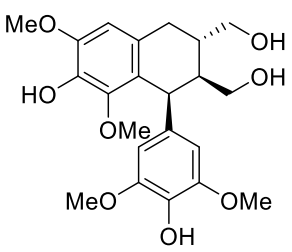

80

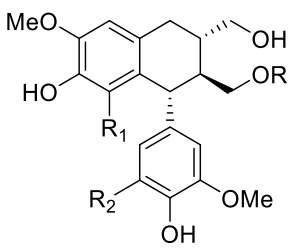

81 R=Glc, R_1=R_2=H
82 R=Glc, R_1=R_2=OMe
83 R=Xyl, R_1=OMe, R_2=OH

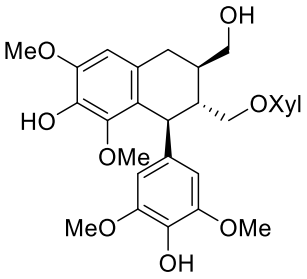

84

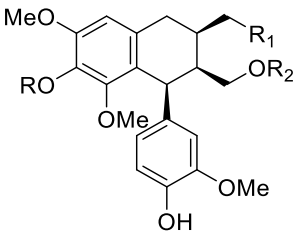

85 R=H, R_1=OH, R_2=Xyl
86 R=Me, R_1=H, R_2=Glc

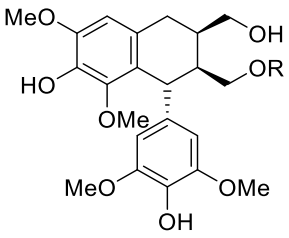

87 R=Xyl
88 R=Rham

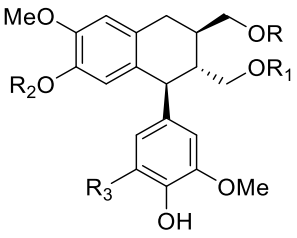

89 R=R_1=R_3=H, R_2=Me
90 R=Glc, R_1=R_3=H, R_2=Me
91 R=R_2=H. R_1=Glc, R_3=OMe

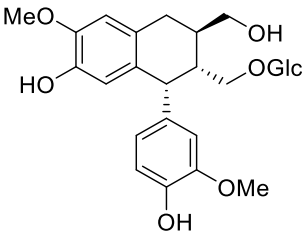

92

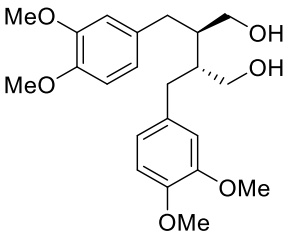

93

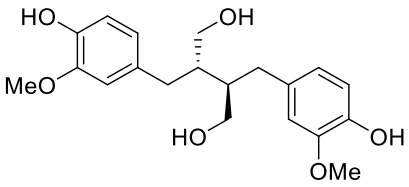

94

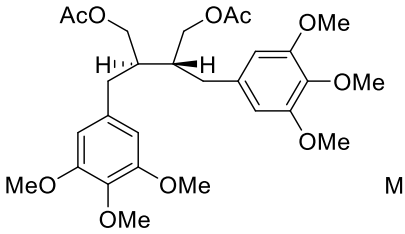

95

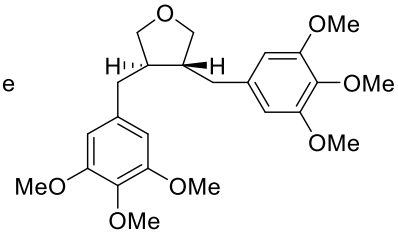

96

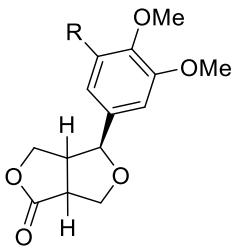

97 R=H
98 R=OMe

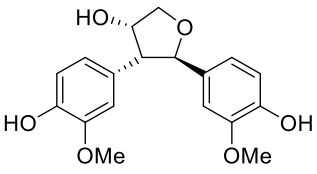

99

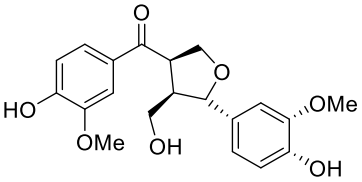

100

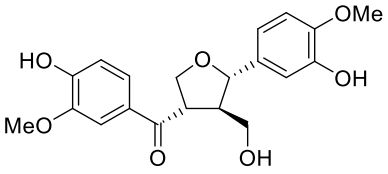

101

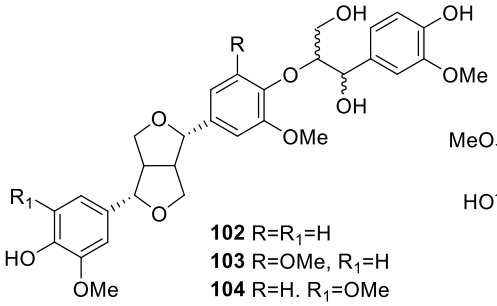

102 R=R_1=H
103 R=OMe, R_1=H
104 R=H. R_1=OMe

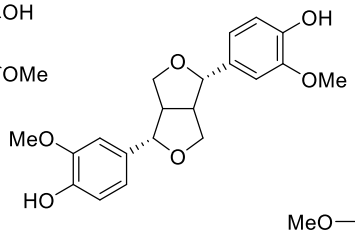

105

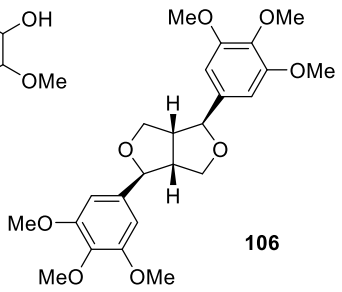

106

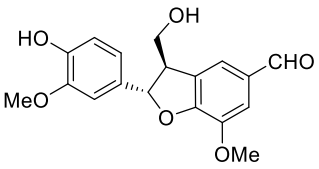

107

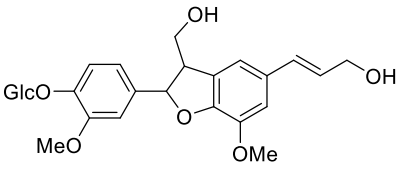

108

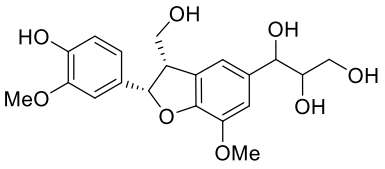

109

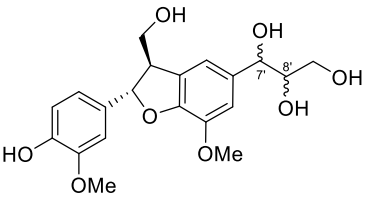

110 (7',8' erythro)
111 (7',8' erythro)
112 (7',8' thero)

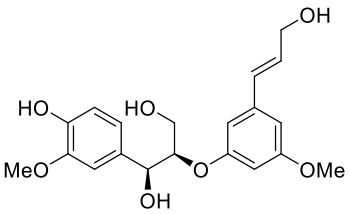

113

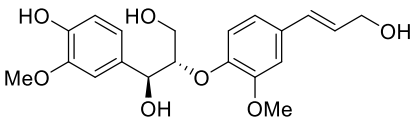

114

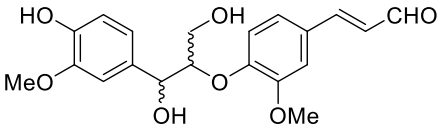

115 (CHO threo-)
116 (CHO erythro-)

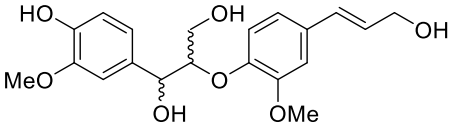

117 (CH_2OH threo-)
118 (CH_2OH erythro-)

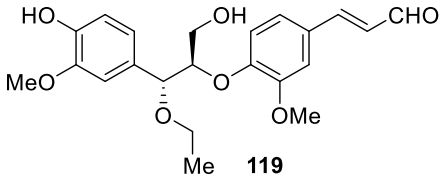

119

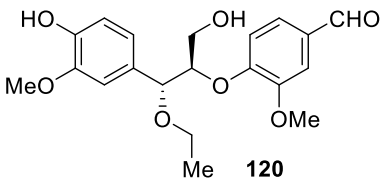

120

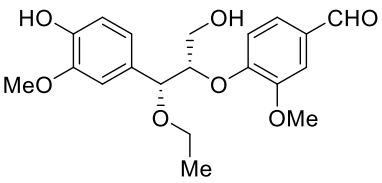

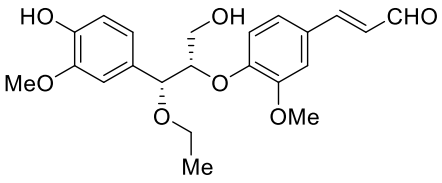

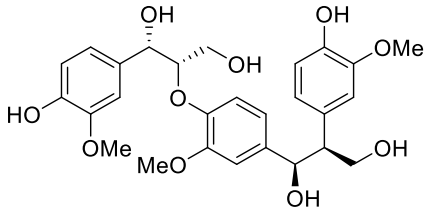

123

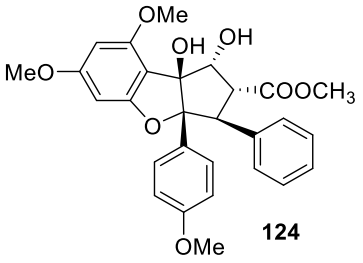

124

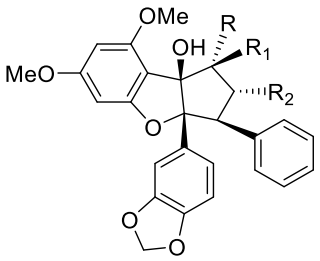

125 R=OH, R_1=H, R_2=COOMe
126 R=OH, R_1=H, R_2=H
127 R=R_2=O, R_3=H

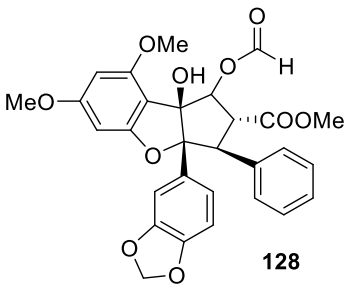

128

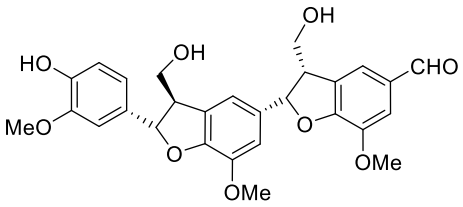

129

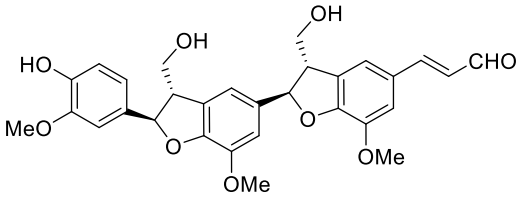

130

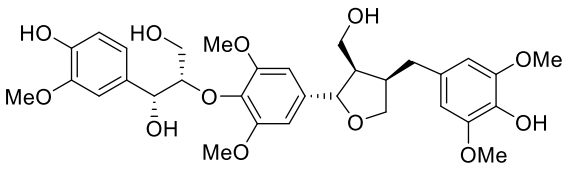

131

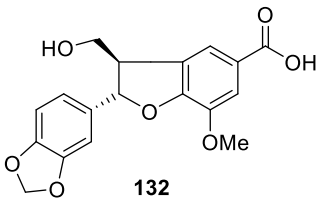

132

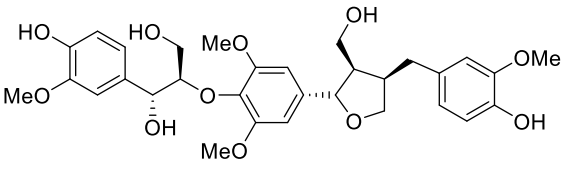

133

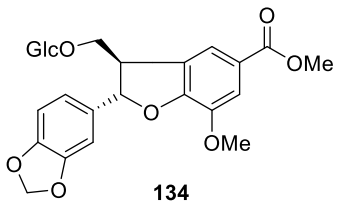

134

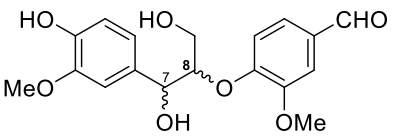

135 (erythro)
136 (threo)

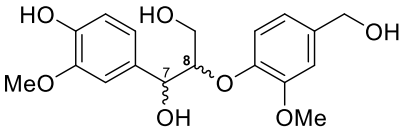

138 (erythro)
139 (threo)

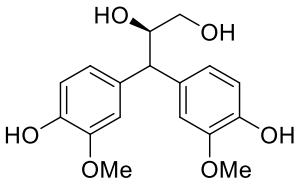

137

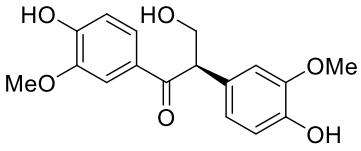

140

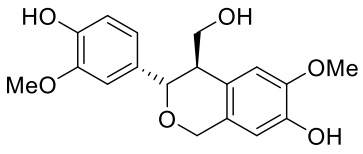

141

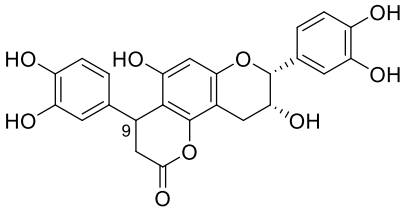

142 9R
143 9S

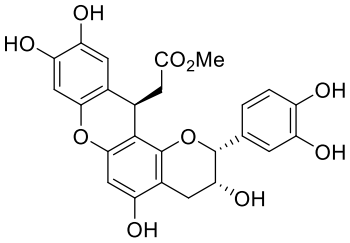

144

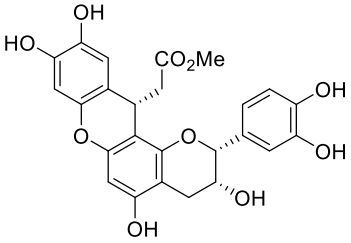

145

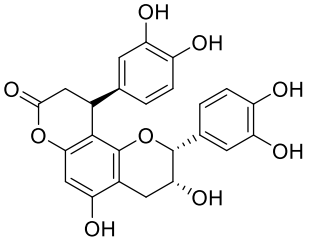

146

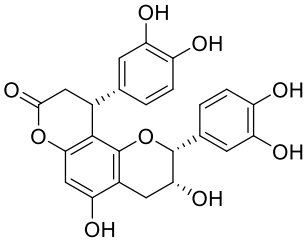

147